Annexin A5 stimulates autophagy and inhibits endocytosis

Ghita Ghislat[1], Carmen Aguado[1,2] and Erwin Knecht[1,2,*]

[1]Laboratorio de Biología Celular, Centro de Investigación Príncipe Felipe, and [2]CIBERER, Avda. Autopista del Saler 16, 46012-Valencia, Spain

*Author for correspondence (knecht@cipf.es)

Summary

Macroautophagy is a major lysosomal catabolic process activated particularly under starvation in eukaryotic cells. A new organelle, the autophagosome, engulfs cytoplasmic substrates, which are degraded after fusion with endosomes and/or lysosomes. During a shotgun proteome analysis of purified lysosomal membranes from mouse fibroblasts, a Ca^{2+}-dependent phospholipid-binding protein, annexin A5, was found to increase on lysosomal membranes under starvation. This suggests a role for this protein, an abundant annexin with a still unknown intracellular function, in starvation-induced lysosomal degradation. Transient overexpression and silencing experiments showed that annexin A5 increased lysosomal protein degradation, and colocalisation experiments, based on GFP sensitivity to lysosomal acidic pH, indicated that this was mainly the result of inducing autophagosome–lysosome fusion. Annexin A5 also inhibited the endocytosis of a fluid-phase marker and cholera toxin, but not receptor-mediated endocytosis. Therefore, we propose a double and opposite role of annexin A5 in regulating the endocytic and autophagic pathways and the fusion of autophagosomes with lysosomes and endosomes.

Key words: Annexin A5, Autophagy, Endocytosis, Lysosome

Introduction

In eukaryotic cells, macroautophagy (hereafter referred to as autophagy) is an important catabolic process for the clearance of intracellular components, including whole organelles, long-lived proteins and other cytosolic molecules (Knecht et al., 2009). The first step in autophagy involves the formation of a flat membrane sac (which in yeast is called the phagophore), the origin of which in mammalian cells is controversial. This structure surrounds cytoplasmic substrates and eventually closes, generating a double-membrane organelle, the autophagosome (Levine and Klionsky, 2004). The endoplasmic reticulum (ER) mainly (Axe et al., 2008; Hayashi-Nishino et al., 2009; Yla-Anttila et al., 2009), and to a lesser extent the mitochondria (Hailey et al., 2010; Mari et al., 2010) and plasma membrane (Ravikumar et al., 2010), appear to contribute proteins and lipids to the forming autophagosome under various situations (Cuervo, 2010). Lysosomes and/or late endosomes are the eventual target of autophagosomes for fusion events, to form autolysosomes containing lysosomal hydrolases that degrade the engulfed material and recycle the breakdown products. The power of yeast genetics has allowed to clarify several steps of the molecular mechanism of this process, and more than 30 evolutionarily conserved autophagy-related proteins have been identified by complementation screening (Klionsky et al., 2003). Some of these proteins are also present in mammalian cells (Knecht et al., 2009), although there are also mammalian-specific proteins involved in autophagy.

Stress conditions, such as starvation, growth factor deprivation or protein aggregation upregulate autophagy to compensate for the lack of amino acids and energy and for other cell stresses and defects (Douglas and Dillin, 2010; Lum et al., 2005; Onodera and Ohsumi, 2005). However, mammalian cells sustain autophagy at a low basal level for the turnover of normally occurring misfolded proteins and damaged molecules and organelles. In mammalian cells, the main autophagy regulators are nutritional and hormonal (Meijer and Codogno, 2006). Thus, in early studies, insulin and amino acids were shown to inhibit autophagy, whereas glucagon activates it. In addition, glucose (which increases autophagy in mammalian cells, in contrast to yeast), vitamins, various growth factors and Ca^{2+} have been also implicated in autophagy regulation.

Ca^{2+} is a universal messenger regulating many physiological functions in cells, such as secretion, contraction, metabolism, gene transcription and death, and it has been implicated also in some pathological processes (Berridge et al., 2003; Perez-Terzic et al., 1995). Regarding its role in autophagy, a pioneering study, exploring the contribution of Ca^{2+} to autophagy, established that stimulation of autophagy depends on its presence within intracellular Ca^{2+}-storage compartments rather than on cytoplasmic Ca^{2+} (Gordon et al., 1993). More recently, it was reported that Ca^{2+} derived from extracellular sources and from ER is a signal for autophagy induction, on the basis of the activation of AMP-activated protein kinase by Ca^{2+}/calmodulin-dependent kinase kinase-β (Hoyer-Hansen et al., 2007). However, other studies have provided evidence that, at least under certain conditions, an increase in cytosolic Ca^{2+} should inhibit autophagy (Williams et al., 2008). In addition to these conflicting conclusions on autophagy regulation, Ca^{2+} has a more well-established role in another closely related lysosomal function, endocytosis, where it is required for efficient fusion

events between late endosomes and lysosomes or autophagosomes (Luzio et al., 2007; Pryor et al., 2000).

While investigating the regulation of the lysosomal degradation of proteins, we carried out a two-dimensional differential gel electrophoresis (2D-DIGE) proteomic study of lysosomal membranes isolated from mouse fibroblasts, to identify proteins whose levels change under conditions of high or low proteolysis in the cells. The proteins on lysosomal membranes that increased under high proteolysis included at least three subunits of the vacuolar ATPase (Esteban et al., 2007) and three Ca^{2+}-dependent phospholipid-binding proteins (annexin A1, annexin A5 and copine 1). In this study, we have concentrated on one of these Ca^{2+}-binding proteins, annexin A5, because it is an abundant annexin with a still unknown intracellular function, and analysed its possible role in lysosomal protein degradation.

Results

Under starvation, annexin A5 translocates from the Golgi complex to lysosomal membranes in a Ca^{2+}-dependent way

To identify proteins involved in the regulation of lysosomal proteolytic pathways, we investigated, by 2D-DIGE and mass spectrometry analysis, lysosomal membranes isolated from NIH3T3 cells incubated in Krebs–Henseleit medium (KH) without (starvation) and with insulin (I), amino acids (AA) or both (IAA). The level of the phospholipid-binding protein annexin A5 was found, along with other proteins on the lysosomal membranes, to change under conditions that produce high (KH), low (IAA) and intermediate (I or AA) proteolysis in the cell (Fig. 1A). As shown in Fig. 1B, levels of annexin A5 in KH decreased after addition of AA or IAA, but not, apparently, after addition of I. This was confirmed by western blot analysis of subcellular fractions enriched in nuclei, mitochondria and lysosomes from NIH3T3 cells incubated under conditions that produce high and low proteolysis. Annexin A5 was located in mitochondrial and lysosomal fractions, and its levels were higher in lysosomes and, with less difference, in mitochondria isolated from cells incubated in KH (Fig. 1C). Consistent with these results, we also found that colocalisation of annexin A5 with a lysosomal protein, cathepsin B (Fig. 1D, see also Fig. 3B, KH and IAA in the histogram) and with LysoTracker Red (see Fig. 3A, two upper panels and KH and IAA in the histogram below), a membrane-diffusible probe that accumulates in acidic organelles, especially lysosomes (Kornhuber et al., 2010), was higher in KH than in IAA. Interestingly, the cellular localisation of annexin A5 is different in the two media. In IAA, annexin A5 had a perinuclear pattern but in KH it was more dispersed and punctate, consistent with its translocation to lysosomes under starvation. Experiments with various markers (Fig. 2) indicated colocalisation of annexin A5 with the Golgi complex and late endosomes, but not with ER and early endosomes. In KH, colocalisation of annexin A5 with the Golgi complex was much weaker, whereas colocalisation with late endosomes was slightly stronger.

In addition, and because annexin A5 is a Ca^{2+}-dependent binding protein, and unpublished results from our laboratory show a rise in intracellular Ca^{2+} levels under starvation (KH) in comparison with fed cells (IAA), we investigated whether the translocation of annexin A5 to lysosomal membranes in starved cells was Ca^{2+} dependent. Thus, an intracellular Ca^{2+} chelator, BAPTA-AM, reduced the colocalisation of annexin A5 with
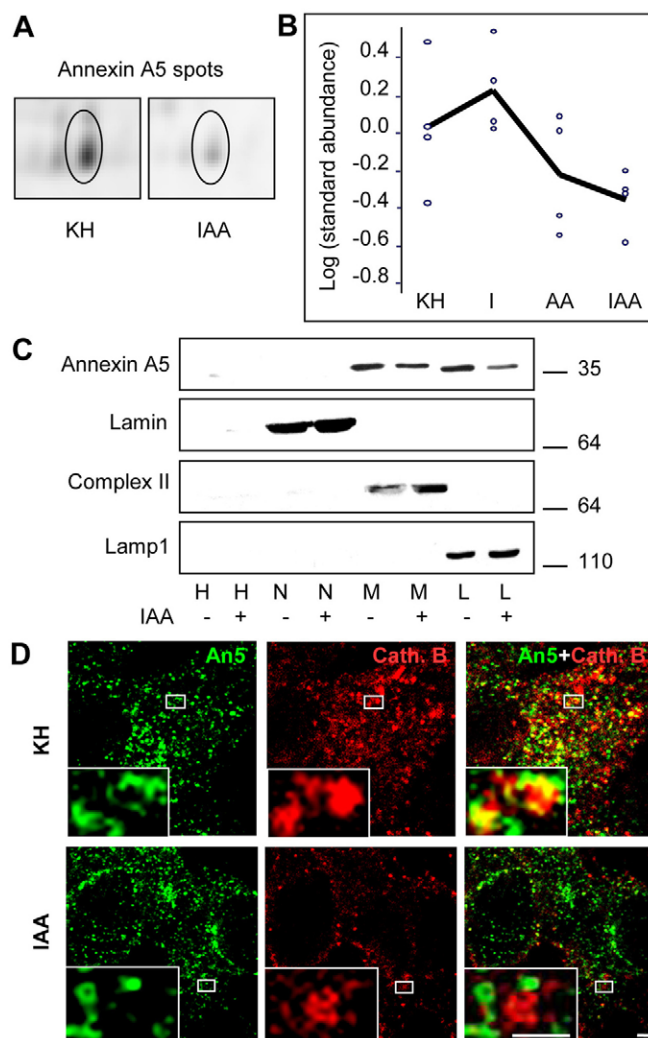

Fig. 1. **Under starvation, annexin A5 translocates to lysosomal membranes.** (**A**) Representative area corresponding to annexin A5 (encircled spots) from 2D gels with proteins (100 µg) from lysosomal membranes isolated from NIH3T3 cells incubated for 4 hours in conditions that produce low (IAA) and high (KH) proteolysis. (**B**) Levels of annexin A5 on lysosomal membranes isolated from cells incubated in Krebs–Henseleit medium without (KH) or with insulin (I), amino acids (AA) or both (IAA). Data are from four independent experiments similar to that shown in A. The line joins the mean values. (**C**) Subcellular fractions were isolated, as described in the Materials and Methods, from NIH3T3 cells incubated for 4 hours in KH (−) or IAA (+). 25 µg protein from each fraction was subjected to SDS-polyacrylamide gel electrophoresis and immunoblotted with antibodies that recognise annexin A5, lamin (nuclear marker), mitochondrial complex II (succinate-ubiquinol oxidoreductase; mitochondrial marker) and lamp1 (lysosomal marker). H, homogenate; N, M, L, nuclear, mitochondrial and lysosomal fractions, respectively. (**D**) Confocal images of NIH3T3 cells incubated for 4 hours in KH (upper panels) or in IAA (lower panels) and immunostained with cathepsin B (Cath. B, middle panels) and annexin A5 (An5, left panels) antibodies (right panels are merged images). Insets: high-magnification images of fusion events. Scale bars: 2.5 µm.

lysosomal markers in the cells incubated in KH medium, whereas in the cells incubated in IAA medium with a Ca^{2+} ionophore, ionomycin, this colocalisation increased (Fig. 3). Taken together, these data suggest that under starvation conditions annexin A5
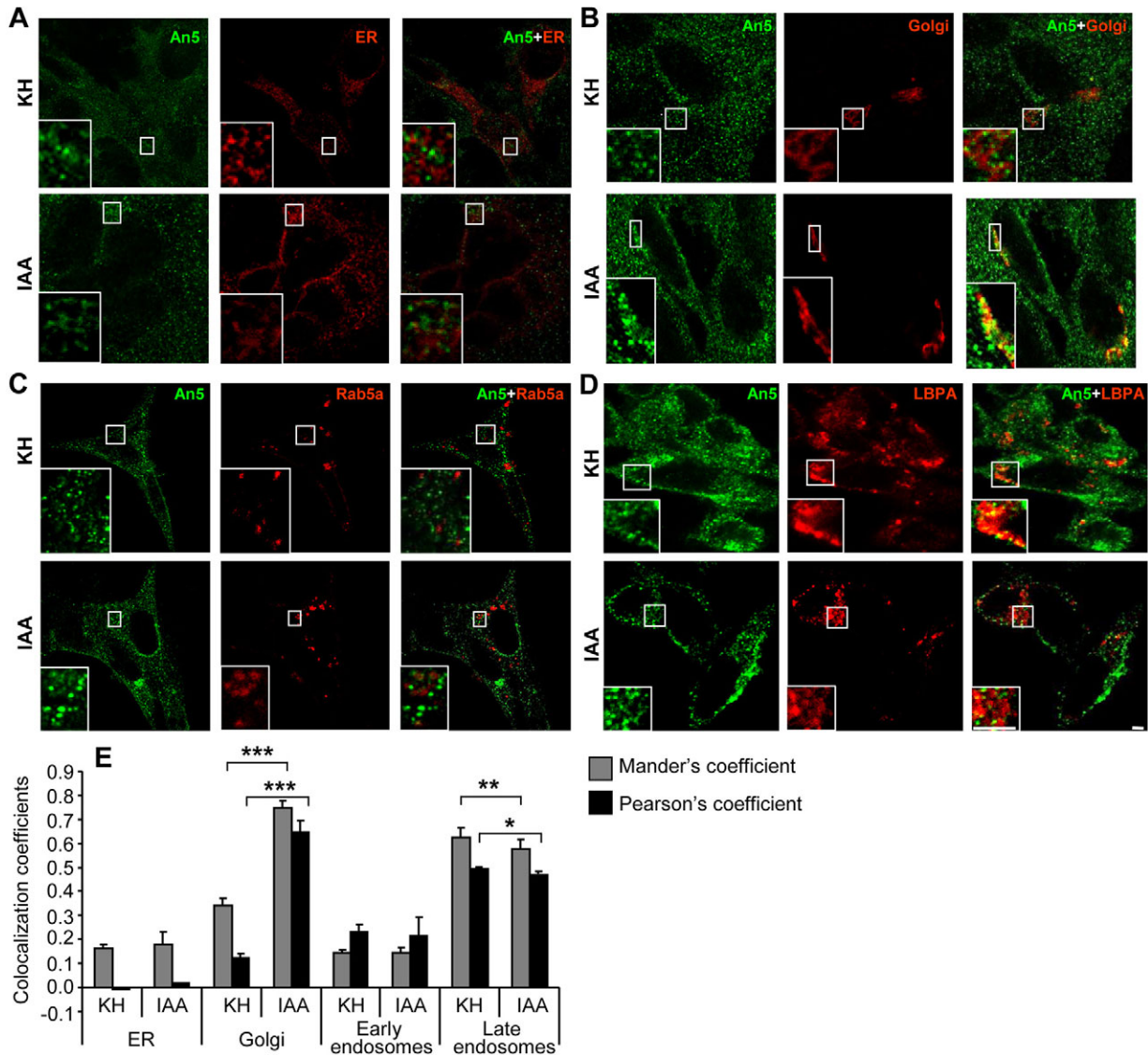
Fig. 2. The intracellular distribution of annexin A5 under high and low proteolysis conditions is different. (A–C) Confocal images of NIH3T3 cells, previously infected with Cell Light-ER (signal sequence of calreticulin and KDEL–RFP; A) or Cell Light-Golgi (*N*-acetylgalactosaminyl-transferase-2–RFP; B) or with Organelle Light-early endosomes (Rab5a–RFP; C). After 4 hours in KH (upper panels) or in IAA (lower panels) medium, cells were immunostained with annexin A5 antibody. (D) Confocal images of NIH3T3 cells incubated for 4 hours in KH (upper panels) or IAA (lower panels) and immunostained with LBPA (middle panels) and annexin A5 (An5, left panels) antibodies. Merged images are shown in the right panels. Scale bars: 5 µm. Insets: high-magnification images of fusion events. (E) Quantification of colocalisations. The analysis, of two independent experiments, was performed as detailed in the Materials and Methods. The graph shows the Mander's colocalisation coefficient (fraction of An5-positive structures overlapping ER, Golgi, Rab5a and LPBA-positive structures; grey bars) and Pearson's correlation coefficient (black bars). Differences between KH and IAA values were found to be statistically significant at *$P<0.05$, **$P<0.005$ and ***$P<0.0005$.

partially translocates from the Golgi complex to lysosomal membranes in a Ca^{2+}-dependent way.

Annexin A5 increases lysosomal protein degradation

In eukaryotic cells under starvation, lysosomes represent the main catabolic compartment. Under these conditions, annexin A5 apparently translocates to lysosomal membranes. Therefore, we investigated its possible role in stimulating lysosomal protein degradation. Because the levels of annexin A5 after overexpression were lower in NIH3T3 than in HEK293T cells, we analyzed wild-type (WT) cells and HEK293T cells transiently transfected with an annexin A5 overexpression vector (hereafter

referred to as A5 vector) or a negative control vector (C– vector). Pulse–chase experiments were carried out to analyze the degradation of long-lived proteins by established procedures (Fuertes et al., 2003a; Mizushima et al., 2010). As shown in Fig. 4, overexpression of annexin A5 increased total (Fig. 4A) and, in particular, lysosomal (Fig. 4B) protein degradation under both high and low proteolysis. This supports a role of annexin A5 in the activation of lysosomal protein degradation. This conclusion was further confirmed by measurements in these cells of the levels of p62, a multifunctional protein that binds LC3-II and is destroyed in lysosomes (Moscat and Diaz-Meco, 2009). As shown in Fig. 4C, overexpression of annexin A5 clearly
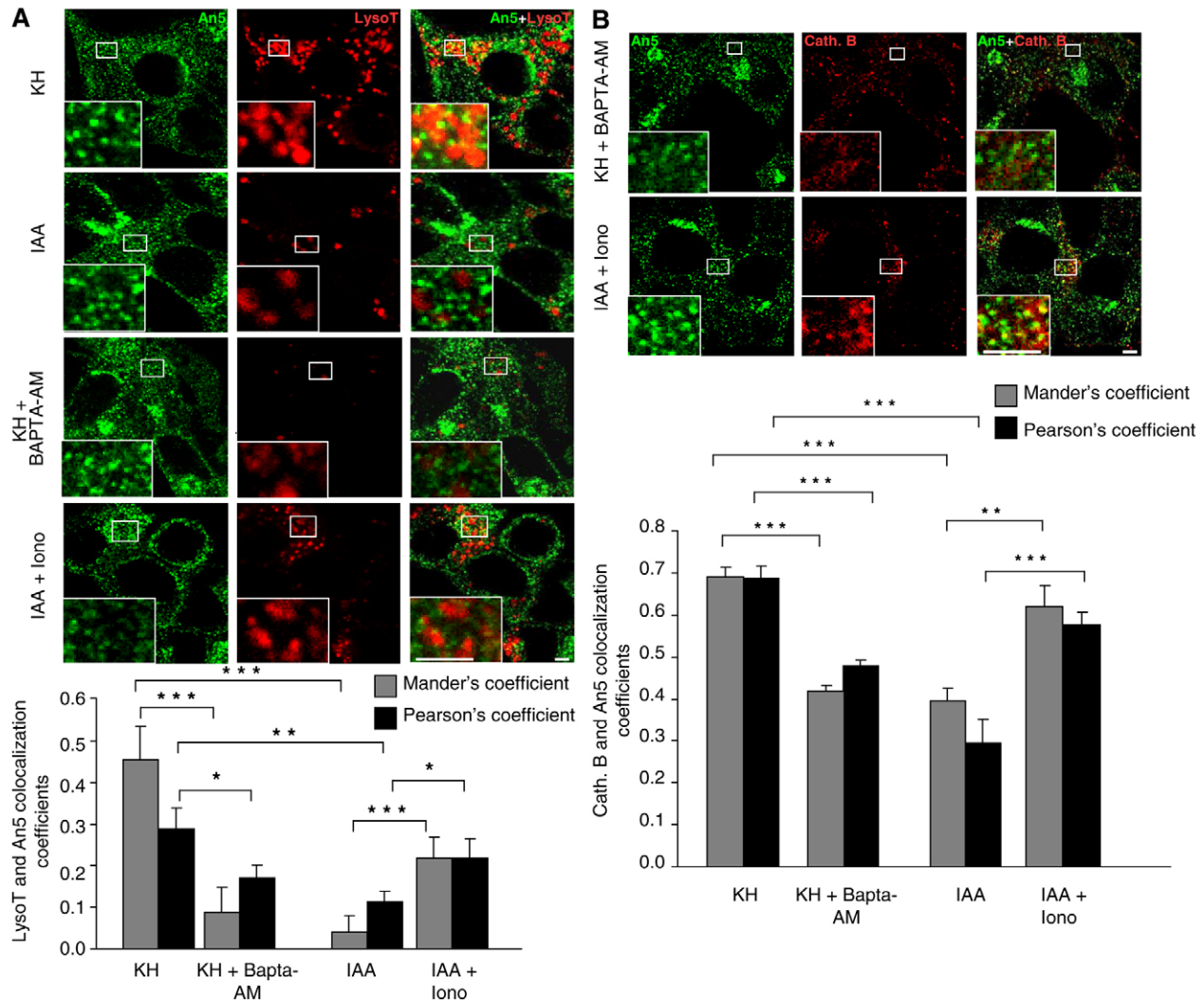
Fig. 3. Colocalisation of annexin A5 with LysoTracker Red and cathepsin B is Ca^{2+} dependent. (A,B) Confocal images of NIH3T3 cells incubated for 4 hours in KH with and without BAPTA-AM (20 µM) or in IAA with or without ionomycin (10 µM) and stained with annexin A5 antibody (An5, left panels), LysoTracker Red (LysoT, middle panels; A) or cathepsin B (Cath. B, middle panels; B). Merged images are shown in the right panels. Scale bars: 2.5 µm. Insets: high-magnification images of fusion events. Quantifications of the colocalisation of annexin A5 with lysosomal markers under the various conditions are shown below. The analysis of two independent experiments was performed as detailed in the legend to Fig. 2E. Differences were found to be statistically significant at *$P<0.05$, **$P<0.005$ and ***$P<0.0005$.

decreases p62 levels, even in the cells incubated in IAA medium, which had more p62 because of its lower degradation, consistent with annexin A5 increasing lysosomal protein degradation. This decrease in p62 levels was prevented when the cells were incubated with bafilomycin A1 (hereafter called bafilomycin), indicating that it depends on lysosomal degradation.

We also investigated, in similar experiments, the effects of silencing annexin A5 with two different short-interfering RNAs (siRNAs), si1 and si2, that target annexin A5 (siA5), using NIH3T3 cells because they express higher levels of this protein. Both siA5 produced a similar silencing of the protein (supplementary material Fig. S1A,B, upper panels) and, therefore, in most of the following assays we show results with one of both, but calculations are shown as the average of the two. Silencing of annexin A5 produced the opposite effect to overexpression; it mainly decreased lysosomal (Fig. 4E) and

moderately decreased total (Fig. 4D) intracellular protein degradation, and this was more evident under high proteolysis conditions (KH). In KH medium, decreased autophagy was also observed with its inhibitor 3-methyladenine (Fig. 4F), but this could not be investigated in IAA medium because under these conditions autophagy is very low and 3-methyladenine has some secondary effects increasing protein degradation, as already observed before by us and by others (Fuertes et al., 2003a; Williams et al., 2008; Wu et al., 2010). The relatively low inhibition of intracellular protein degradation by annexin A5 silencing ($14.6\pm2.3\%$ in KH) can perhaps be explained by redundancy, because, for example, cosilencing of annexin A5 and copine 1 increased considerably ($\sim40.5\pm6.5\%$ in KH) this inhibition (our unpublished results). In addition, we found that in IAA and also in KH, silencing of annexin A5 raised p62 levels (Fig. 4G). However, in bafilomycin-treated cells, in
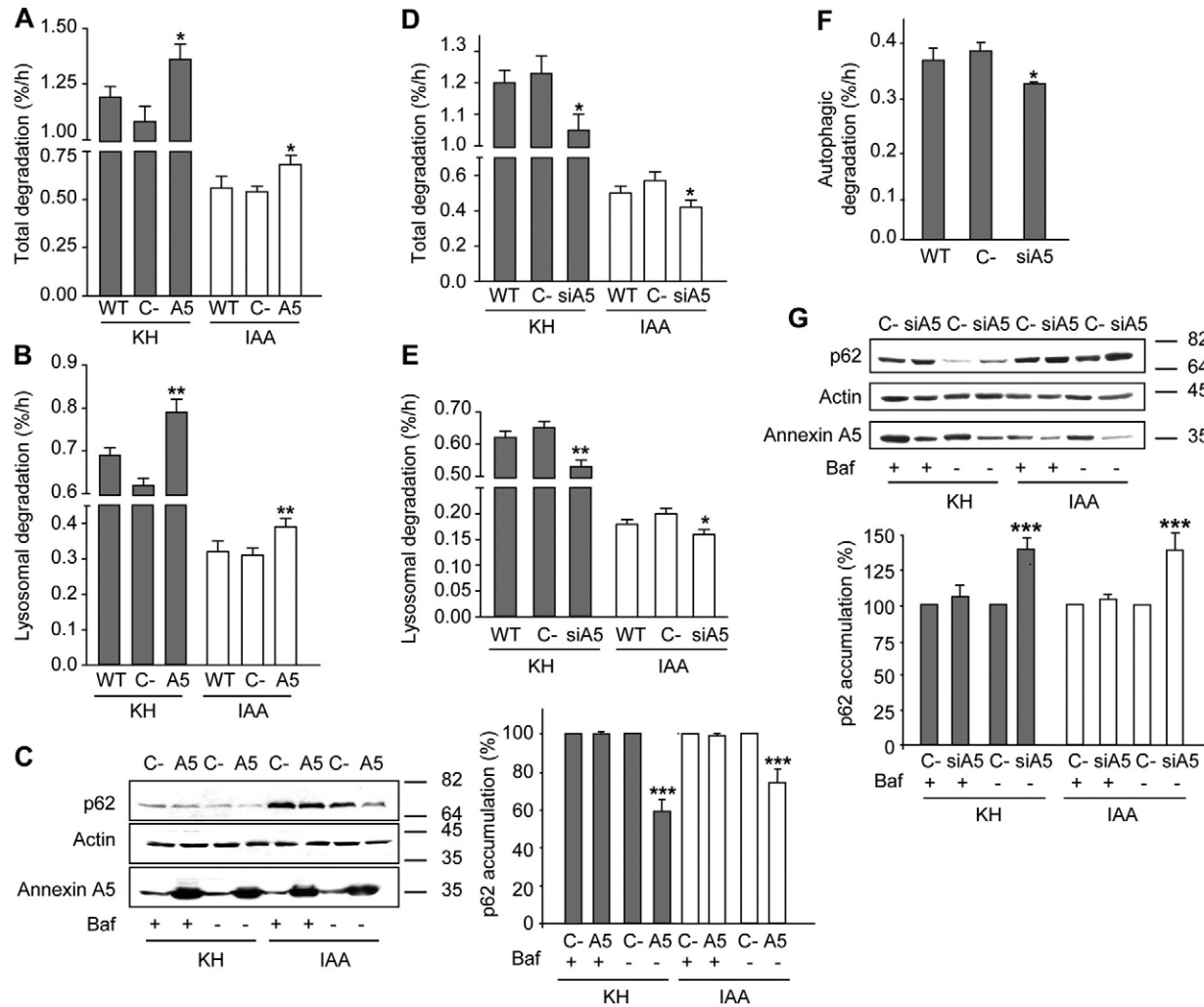
Fig. 4. Annexin A5 increases lysosomal protein degradation. (**A,B**) Overexpression of annexin A5 increases lysosomal protein degradation. Exponentially growing HEK293T cells [wild type (WT) and transiently transfected with C– or A5 vector] were metabolically labelled with [^{3}H]valine for 48 hours, chased for 24 hours and then switched for 4 hours to KH or IAA medium. Total (A) and lysosomal (B) protein degradations were calculated as described in the Materials and Methods. Results from three separate experiments with duplicated samples are shown as the percentage of the labelled proteins that were degraded per hour under the different conditions. (**C**) Cells treated and incubated as above, with and without bafilomycin A1 (Baf, 500 nM), were subjected to immunoblotting with p62, actin (as a loading control) and annexin A5 (to show overexpression) antibodies. Densitometric measurements of the p62 bands shown in the histogram on the right were normalised to the corresponding actin bands and expressed as a percentage of the corresponding negative control (C–) values. (**D–F**) Silencing of annexin A5 decreases lysosomal protein degradation. Exponentially growing NIH3T3 cells (WT and treated with C– or siA5 vector) were labelled and incubated as above. Total (D), lysosomal (E) and autophagic (F) degradations were calculated as indicated in Materials and Methods. Values are the means and s.d. from ten independent experiments with duplicated samples. (**G**) NIH3T3 cells, treated and incubated as above, were subjected to immunoblotting with p62, actin and annexin A5 antibodies. Densitometric measurements of the p62 bands were normalised to the corresponding actin bands and are shown in the histogram below. Data are expressed as in C and are the means and s.d. of four independent experiments. Differences from the respective control values in the different histograms were found to be statistically significant at *$P<0.05$, **$P<0.005$ and ***$P<0.0005$.

which p62 levels increased, annexin A5 knockdown caused no further increase. This indicates that the decrease in the levels of p62 depends on lysosomal degradation and that this process is partially defective under annexin A5 silencing. Therefore, all these results are consistent with annexin A5 increasing lysosomal protein degradation.

Annexin A5 enhances autophagosome maturation

Under starvation, autophagy is activated to maintain amino acids and energy levels in the cell and becomes the main lysosomal degradation pathway (Knecht et al., 2009; Levine and Klionsky,

2004). Therefore, we investigated more specifically the effect of annexin A5 on autophagy with its well-established marker LC3-II. For overexpression experiments we used, as above, transiently transfected HEK293T cells with A5 or C– vector. Overexpression of annexin A5 decreased LC3-II levels (Fig. 5A, high exposure blot). This was also observed using HEK293T cells with stable expression of eGFP–LC3: overexpression of annexin A5 decreased the number of fluorescent puncta under high and low proteolysis conditions (Fig. 5B). Because overexpression of annexin A5 increases lysosomal proteolysis, the observed decrease in LC3-II levels cannot be due to a reduced
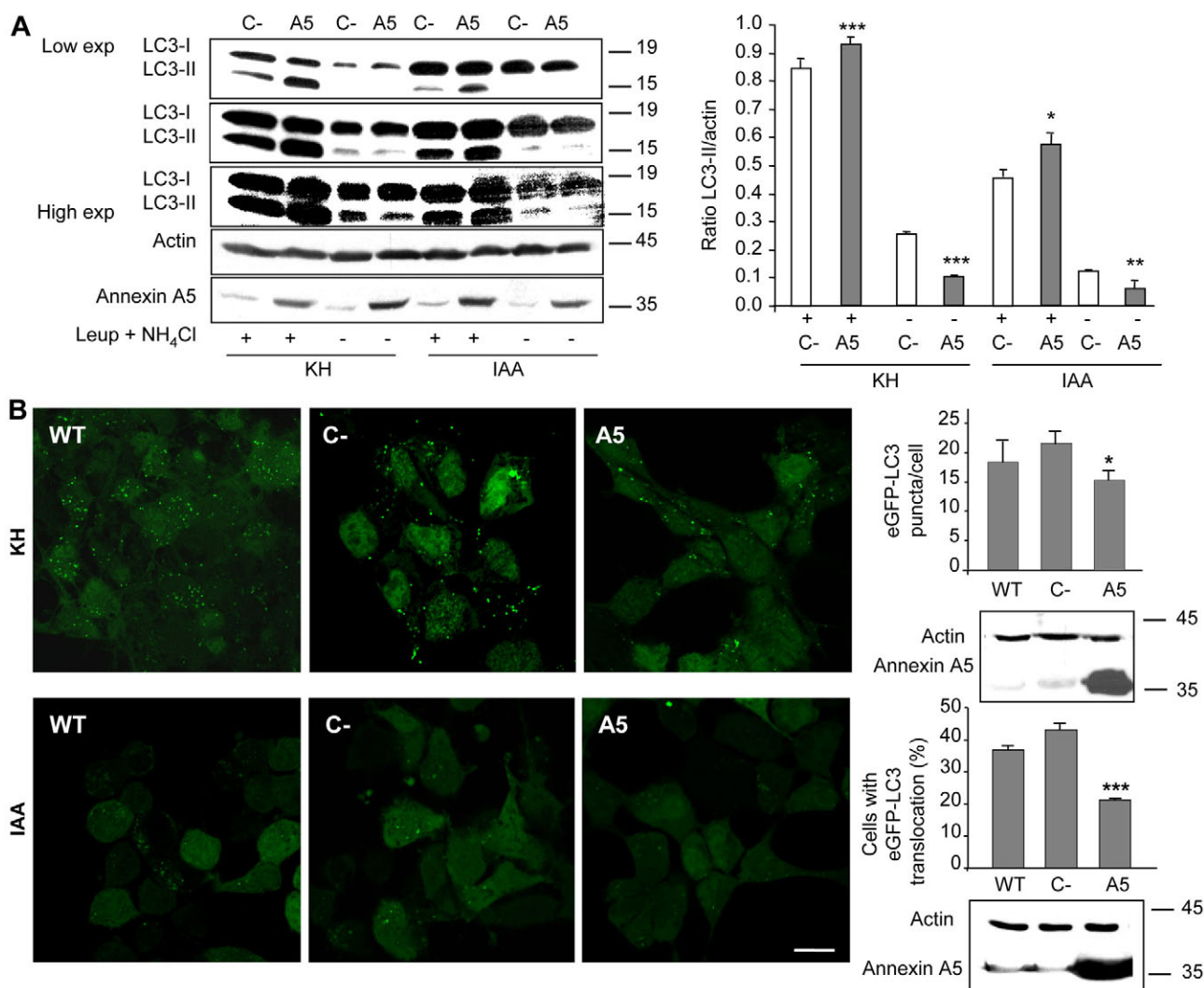
Fig. 5. Annexin A5 overexpression increases autophagic flux. (**A**) HEK293T cells were transiently transfected with A5 or C– vector as in Fig. 4A–C. After 48 hours, the cells were incubated for 4 hours in KH or IAA medium with or without leupeptin (Leup, 100 µM) and NH$_4$Cl (20 mM). Then, the cells (75 µg protein) were subjected to immunoblotting, with various exposures (exp), using antibodies that recognise LC3 (-I and -II), actin and annexin A5. The histogram on the right shows densitometric measurements of the ratio of LC3-II to actin bands from six independent experiments. (**B**) HEK293T cells with stable expression of eGFP–LC3 were transiently transfected and incubated as in A and examined using a confocal microscope. WT NIH3T3 cells are also shown. Scale bar: 10 µm. The number of eGFP–LC3 puncta/cell (KH) or the percentage of cells with fluorescent dots (IAA, cells containing more than five dots were considered positive) were determined in two independent experiments (at least 150 cells per condition) and results are shown on the right. Actin and annexin A5 levels are also shown below. Differences from negative control (C–) values in the histograms in A and B were found to be statistically significant at *$P<0.05$, **$P<0.005$ and ***$P<0.0005$.

autophagosome formation but instead reflects an enhanced conversion of autophagosomes into autolysosomes. Under inhibition of the degradation of LC3-II in autolysosomes using various treatments (Codogno and Meijer, 2005) the levels of LC3-II are indicative of the formation rate of autophagosomes (Levine and Klionsky, 2004; Lum et al., 2005; Mizushima et al., 2010). Using leupeptin and ammonium chloride, a treatment with the same effect on LC3-II accumulation as bafilomycin (Esteve et al., 2010), to inhibit lysosomal degradation, we found that overexpression of annexin A5 not only does not decrease LC3-II levels, but it even produces a substantial increase (Fig. 5A, low exposure blot). Thus, annexin A5 probably also increases autophagosome formation, but this effect should be less important, because in the absence of lysosomal inhibitors LC3-II levels decrease.

Silencing of annexin A5 with two different siRNAs in NIH3T3 cells incubated in KH or in IAA resulted in accumulation of the autophagosome-associated protein LC3-II in the absence of lysosomal inhibitors (lower panel in supplementary material Fig. S1A). This accumulation most probably occurs because of a decreased degradation of LC3-II in the absence of annexin A5 due to an inhibition of autophagosome–lysosome fusion, as suggested in the overexpression experiments. However, the accumulation of LC3-II was also observed in the presence of lysosomal inhibitors (especially in IAA, lower panel in supplementary material Fig. S1B). This was not a cell-type-specific effect, because similar results were obtained with both siRNAs in HEK293T cells (supplementary material Fig. S1C,D). Fig. 6A includes, on the right, the densitometric analysis of
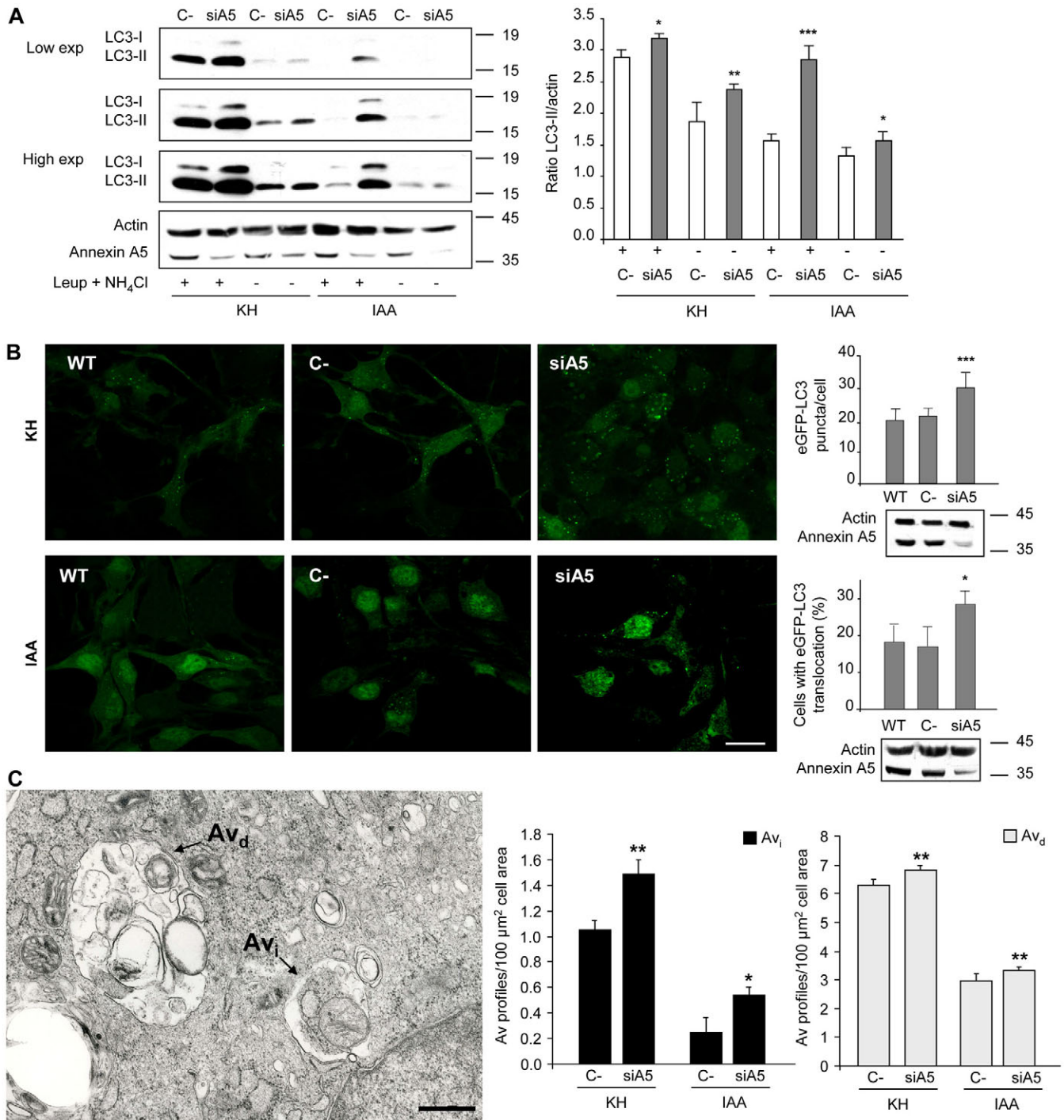
Fig. 6. Silencing of annexin A5 increases the accumulation of autophagosomes. (**A**) NIH3T3 cells were transfected with annexin A5 (siA5) or a negative control (C–) siRNA. After 72 hours cells were incubated, immunoblotted and subjected to densitometric analysis as described in the legend to Fig. 5A. The histogram on the right shows the ratio of LC3-II to actin bands from eight independent experiments. (**B**) NIH3T3 cells stably expressing eGFP–LC3 (WT) were transfected with siA5 or C– siRNA for 72 hours, incubated for 4 hours in KH or in IAA medium and then examined using a confocal microscope. Scale bar: 10 μm. The number of eGFP–LC3 puncta per cell (KH) or the percentage of cells with fluorescent dots (IAA) in two different experiments were determined as described in the legend to Fig. 5B and results are shown on the right. Actin and annexin A5 levels are also shown below. (**C**) Representative electron micrograph of NIH3T3 cells transfected with siA5 incubated in KH medium for 4 hours showing early (Av_i) and late (Av_d) autophagic vacuoles. Scale bar: 0.5 μm. The histograms on the right show the amounts of Av_i and Av_d, in cells transfected with C– or siA5 siRNAs, incubated in KH or in IAA medium, determined by morphometry in two different experiments. Differences from negative control (C–) values in all the histograms were found to be statistically significant at *$P<0.05$, **$P<0.005$ and ***$P<0.0005$.

various experiments similar to the silencing experiment shown on the left. The observed increase in autophagic vacuoles in the cells incubated without lysosomal inhibitors was further confirmed using NIH3T3 cells that stably expressed eGFP–LC3 (Fig. 6B). Also, knockdown of annexin A5 increased the fractional volume of early (Av_i) and late (Av_d) autophagic vacuoles (Fig. 6C), and this increase was proportionally higher for Av_i (1.42× in KH and 2.16× in IAA) than for Av_d (1.08× in KH and 1.13× in IAA). These results suggest again a role of annexin A5 in autophagosome maturation. However, the observed accumulation of LC3-II after silencing of annexin A5 in the presence of lysosomal inhibitors remains to be explained. This is discussed below.

Annexin A5 induces autophagosome delivery to lysosomes
To confirm with a different procedure that annexin A5 increases autophagic flux, as suggested in the above experiments, we used a flow cytometric assay based on the loss of eGFP fluorescence when eGFP–LC3 bound to autophagosomal membranes is delivered to lysosomes for degradation (Shvets and Elazar, 2009). As expected, if lower eGFP–LC3 fluorescence is due to an increased autophagic flux, fluorescence was lower in starvation medium (KH) than in IAA, and this decrease was blocked with wortmannin, which inhibits autophagy (Fig. 7A). Annexin A5 overexpression induces a decay in eGFP–LC3 fluorescence (Fig. 7B), indicating an enhanced delivery of eGFP–LC3 to the lysosomal compartment, whereas annexin A5 silencing increased

this fluorescence (Fig. 7C). These results are in agreement with the LC3 western blot experiments and support the involvement of annexin A5 in the delivery of autophagosomes to lysosomes.

To further confirm the effect of annexin A5 on autophagosome maturation, we used HEK293T and NIH3T3 cells stably expressing an mRFP–GFP–LC3 tandem reporter that has been found to be useful to trace autophagosome maturation (Kimura et al., 2007). Hence, within lysosomes eGFP–LC3 fluorescence is quenched because of the sensitivity of GFP to acidic environments, whereas mRFP–LC3 fluorescence is more stable upon acidification. Thus, autophagosomes with a physiological pH show both red and green fluorescence, whereas the latter is lost in autolysosomes with an acidic pH. Overexpression of annexin A5 in HEK293T cells led to a rise in vesicles with red fluorescence in both KH and IAA media (Fig. 8A), indicating increased autophagosome maturation. By contrast, the relative proportion of vesicles with yellow fluorescence increased in annexin-A5-silenced NIH3T3 cells incubated in both media (Fig. 8B). These results suggest again a role of annexin A5 in autophagosome maturation. Moreover, changing the endogenous levels of annexin A5 (by overexpression or silencing) did not affect the proteolytic activities of extracts of cells within a wide range of pHs (3.0–8.0), including those that are optimal for lysosomes (supplementary material Fig. S2A,B), or the intralysosomal pH (supplementary material Table S1). Therefore, although we cannot totally exclude an effect of annexin A5 on the
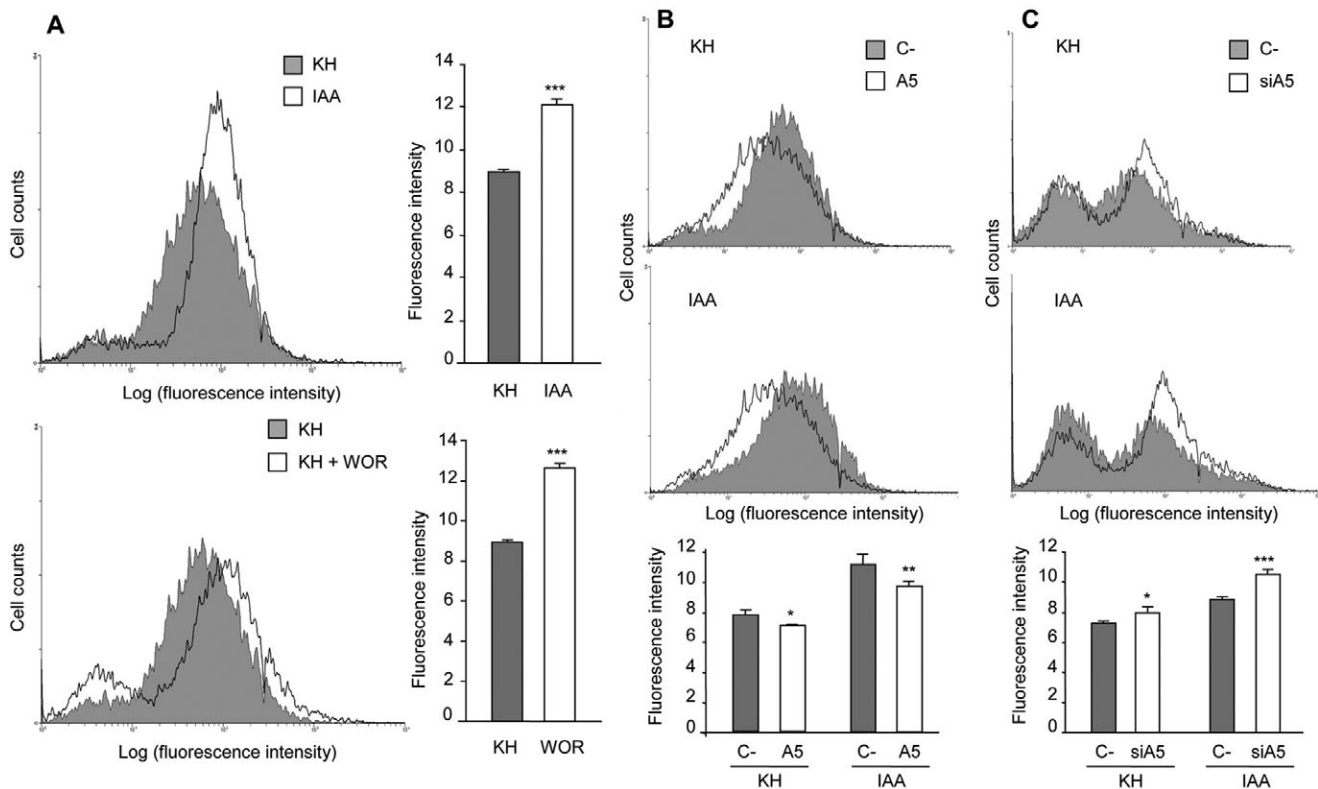

Fig. 7. Annexin A5 promotes autophagosome delivery to lysosomes. NIH3T3 cells stably expressing eGFP–LC3 were incubated under the indicated conditions, and the fluorescence intensity of eGFP in the cells was measured by flow cytometry. Histograms show the mean values of each measurement. (A) Cells were incubated for 4 hours under conditions that produce low (IAA) or high (KH) proteolysis, without or with (Pillay et al., 2002) 100 nM wortmannin (+ WOR). (B,C) HEK293T and NIH3T3 cells stably expressing eGFP–LC3 were, respectively, transfected with C– or A5 vector (B) or C– or siA5 siRNA (C). Values are the means and s.d. from at least four separate experiments with duplicated samples. Differences from negative control (C–) values were found to be statistically significant at *P<0.05, **P<0.005 and ***P<0.0005.
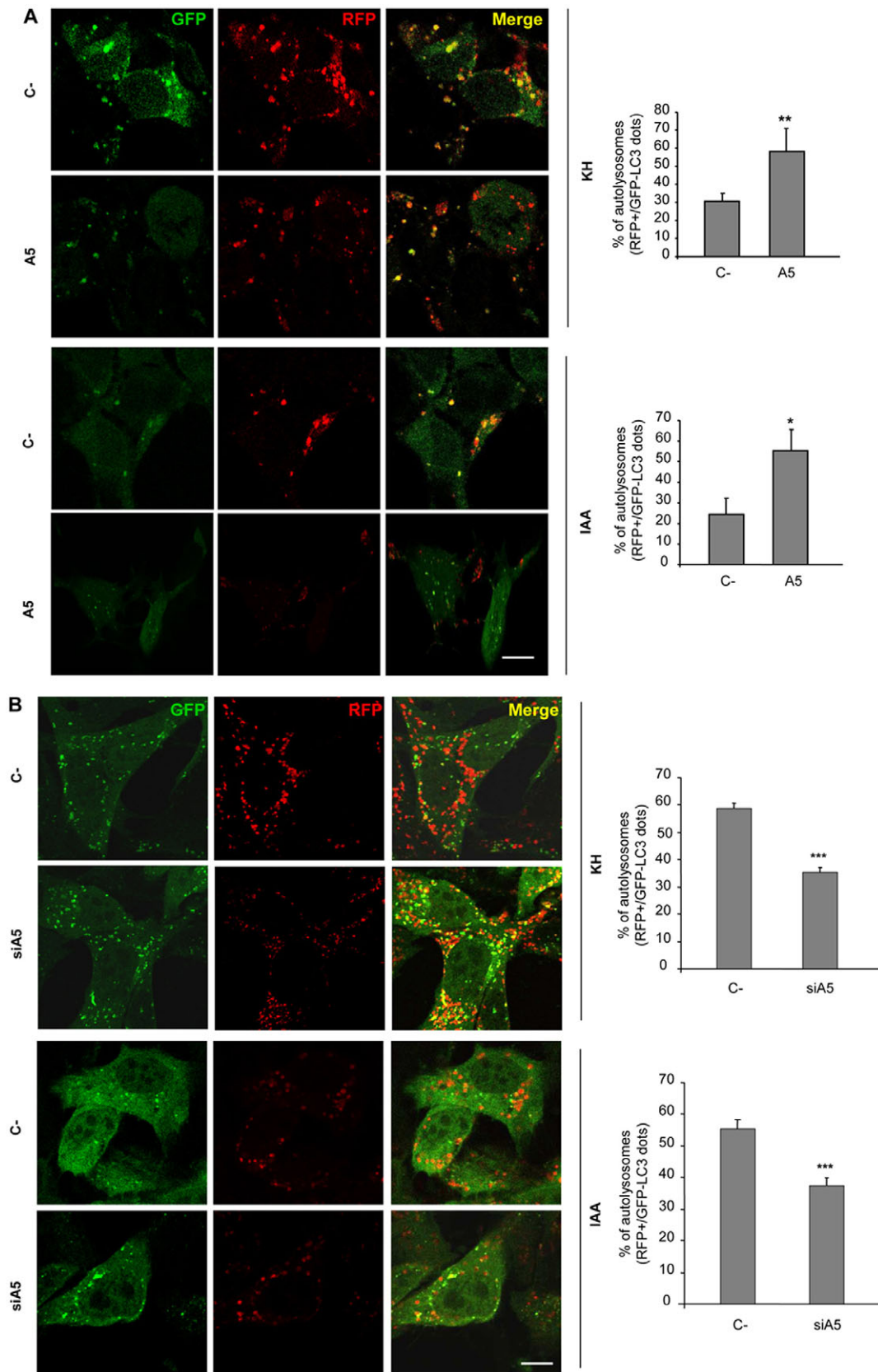
Fig. 8. Annexin A5 promotes autophagosome maturation. (**A**) HEK293T or NIH3T3 cells stably expressing an mRFP–GFP–LC3 construct were seeded on glass coverslips and transfected for (**A**) 48 hours with A5 or C– plasmid or (**B**) for 72 hours with siA5 or C– siRNA. Then, the cells were incubated for 4 hours in KH or in IAA medium and subsequently fixed and analysed by confocal microscopy. The histograms on the right show the percentage of autolysosomes in the cells incubated under the various conditions calculated from three different experiments. Differences from negative control (C–) values were found to be statistically significant at *$P<0.05$, **$P<0.005$ and ***$P<0.0005$. Scale bars: 5 μm.

lysosomal degradative capacity, most data support a major role for it in increasing the fusion of autophagosomes with lysosomes.

Because annexin A5 does not change intralysosomal pH, we also quantified the LysoTracker Red labelling by flow cytometry. Annexin A5 overexpression (Fig. 9A) slightly increased LysoTracker Red staining, especially in IAA. Therefore, it appears that annexin A5 is involved in the maturation of autophagosomes. However, silencing of annexin A5 produced the same effect (Fig. 9B) and this remains to be explained.

Annexin A5 is a negative regulator of endocytosis and of amphisome formation

Because annexin A5 appears to increase autophagy, it is surprising that its silencing also increases lysosomal mass. Lysosomes are ubiquitous degradation organelles that receive their substrates through either endocytosis or autophagy. Thus, we considered the possibility that the increase in LysoTracker Red staining under annexin A5 silencing was due to enhanced endocytic flux. Therefore, we measured the effect of annexin A5 on the internalisation of FITC–dextran, a fluid phase endocytosis marker. Overexpression of annexin A5 reduced FITC-dextran uptake (Fig. 10A), whereas silencing strongly increased its uptake (Fig. 10B). These results indicate that annexin A5 is a negative regulator of fluid phase endocytosis. Similar, but less

evident, effects were obtained with cholera toxin: overexpression and silencing of annexin A5 decreased (Fig. 10C) and increased (Fig. 10D), respectively, its endocytosis. By contrast, annexin A5 has no apparent effect on receptor-mediated endocytosis (supplementary material Fig. S3). Therefore, because annexin A5 increases autophagosome delivery to lysosomes and decreases endocytosis at the same time, these effects can probably account for the enhanced lysosomal mass observed under both overexpression (increased autophagic maturation) and knockdown (increased endocytic uptake) of this protein.

A last observation that remains to be explained is why annexin A5 silencing increases LC3-II levels in the presence of lysosomal inhibitors. Because annexin A5 silencing also increases endocytosis, we considered that the accumulation of LC3-II could be a secondary effect produced by an enhanced fusion of autophagosomes with late endosomes. Therefore, a colocalisation analysis was carried out in NIH3T3 cells using antibodies that recognise LC3, as marker of autophagosomes, and lysobisphosphatidic acid (LBPA), as a marker of late endosomes. The use of eGFP–LC3 was not possible here because the low pH quenches the fluorescent signal of GFP (Kimura et al., 2007). As shown in Fig. 11A–C, annexin A5 silencing increases in fact the colocalisation of LBPA with LC3 and, thus, the formation of the amphisomes, which do not
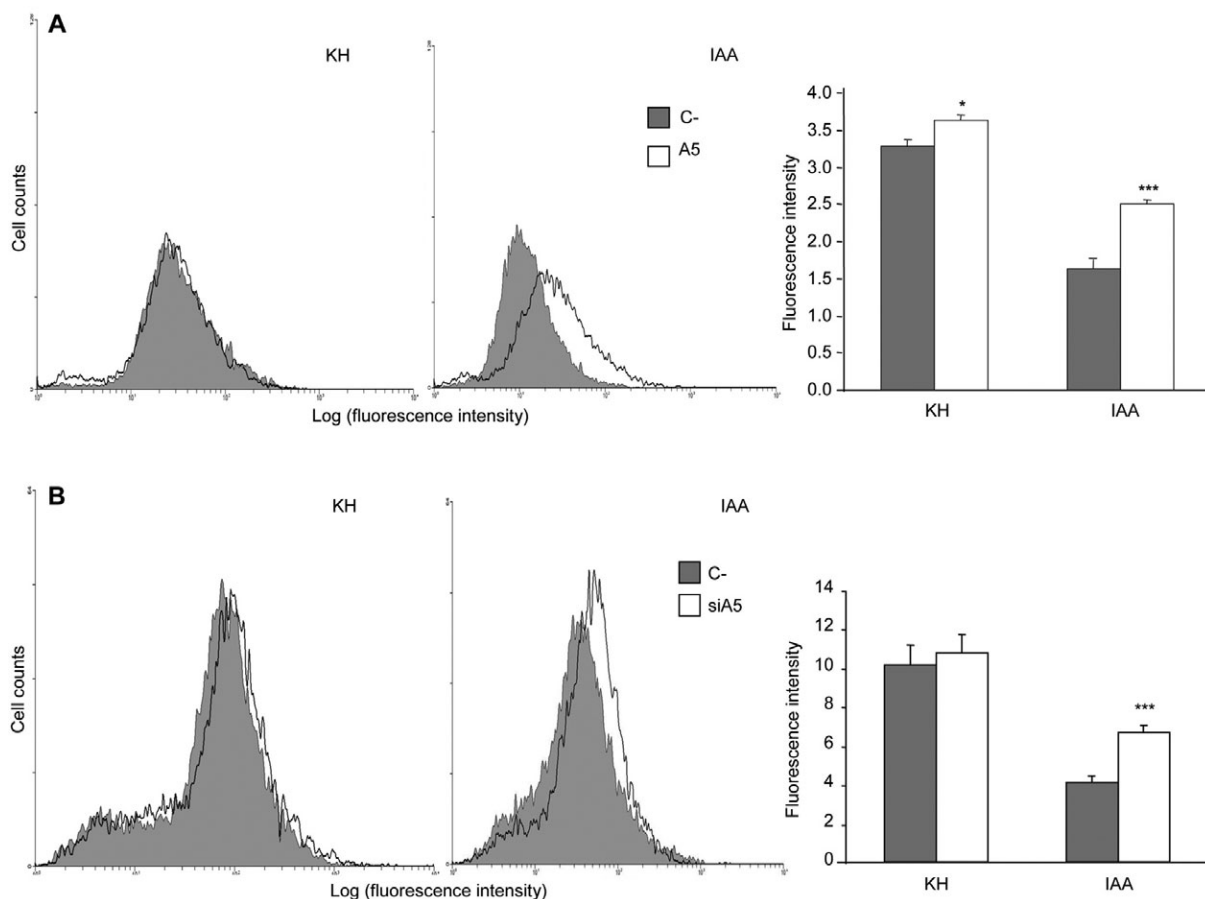

Fig. 9. Both silencing and overexpression of annexin A5 increase lysosomal mass. NIH3T3 cells transfected with C– or A5 vector (**A**) or HEK293T cells transfected with C– or siA5 siRNA (**B**) were incubated for 4 hours in KH or IAA medium in the presence of LysoTracker Red (75 nM). LysoTracker Red fluorescence was analyzed by quantitative flow cytometry (10,000 events). In the histograms on the right, the results shown are the means and s.d. from two separate experiments. Differences from negative control values (C–) were found to be statistically significant at $*P<0.05$ and $***P<0.0005$.
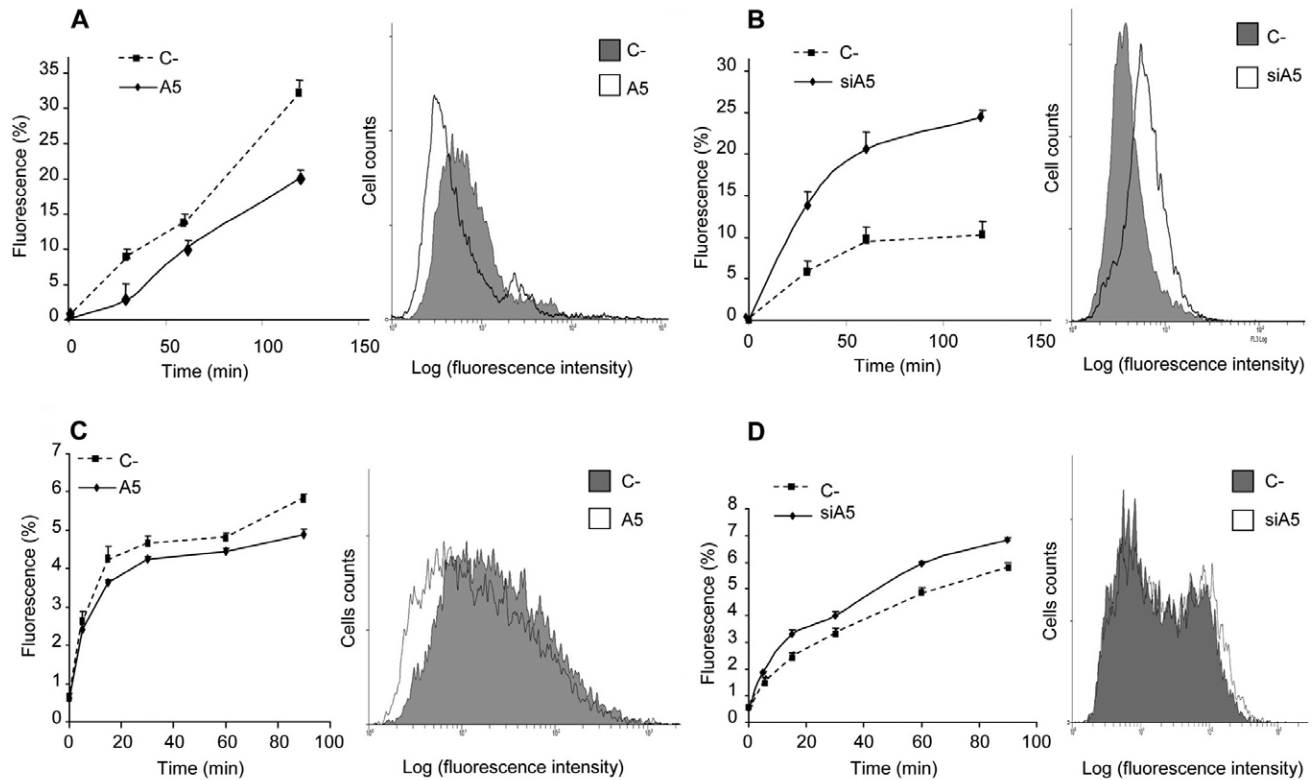
Fig. 10. Annexin A5 inhibits fluid phase and cholera toxin endocytosis. (**A,B**) Quantitative flow cytometry (10,000 events) of FITC–dextran (1 mg/ml) internalisation in HEK293T cells transfected with C– or A5 vector (A) and in NIH3T3 cells transfected with C– or siA5 siRNA (B). (**C,D**) Similar experiments were carried out with Alexa-Fluor-488–cholera-toxin-subunit-B (1.5 μg/ml) in HEK293T cells transfected with C– or A5 vector (C) and in NIH3T3 cells transfected with C– or siA5 siRNA (D). All experiments were carried out for 5 seconds at 4°C (to evaluate the membrane bound marker), for 30, 60 and 120 minutes at 37°C for fluid phase endocytosis, and for 5, 15, 30, 60 and 90 minutes at 37°C for cholera toxin B endocytosis. In A–D, values on the *y*-axis of the graphs indicate the percentage fluorescence in arbitrary units of viable cells, as assessed by propidium iodide staining (1 μg/ml). Values are the means and s.d. from six separate experiments.

degrade LC3-II as efficiently as autolysosomes (Pillay et al., 2002). This could explain the relatively low effect of annexin A5 knockdown in the pulse–chase experiments shown in Fig. 4D–F and the observed accumulation of LC3-II in annexin A5 silenced cells in the presence of lysosomal inhibitors.

Interestingly, quantification of the LBPA-stained area showed an important increase under annexin A5 knockdown (Fig. 11D), in agreement with the negative involvement of this protein in the endocytic pathway.

In summary, all the results presented here support new intracellular roles of annexin A5. First, annexin A5 facilitates the autophagic flux, increasing the fusion of autophagosomes with lysosomes but not with late endosomes. Second, annexin A5 is a negative regulator of some endocytic pathways and, therefore, its silencing increases, whereas its overexpression decreases, them.

Discussion

Although, in the last few years, numerous contributions have produced a better understanding of the mechanisms of autophagy, crucial questions remain unanswered. In autophagy, formation of autophagosomes and fusion at later stages with lysosomes and/or endosomes are both important for autophagic flux (Noda et al., 2009; Xie and Klionsky, 2007). Our results demonstrate the

involvement of annexin A5, a Ca^{2+}-binding protein, in this process. This annexin belongs to a superfamily of structurally related, Ca^{2+}-sensitive proteins that bind to negatively charged phospholipids, establishing specific interactions with other lipid microdomains. They are present in all eukaryotic cells and share a common folding motif, the 'annexin core', with Ca^{2+}- and lipid-binding sites. Annexins participate in a variety of intracellular processes, ranging from the regulation of membrane dynamics to cell migration, proliferation and apoptosis (Monastyrskaya et al., 2009). Annexin A5, one of the most abundant annexins in mammalian cells, has a hitherto unknown function within the intracellular environment, although it has been found to modulate the activities of protein kinase C as well as phospholipase A by interfering with their binding to negatively charged phospholipids and Ca^{2+} (Russo-Marie, 1999). Furthermore, an anti-thrombotic property has been proposed for annexin A5 by shielding phospholipids, especially phosphatidylserine, and thereby blocking their availability for coagulation reactions (Cederholm and Frostegard, 2007).

The results shown here indicate that annexin A5 migrates to lysosomal membranes under starvation and, because this is one of the best characterised stimuli of autophagy (Knecht et al., 2009), we hypothesised a possible involvement of annexin A5 in this process. We found that starvation provokes a translocation of this
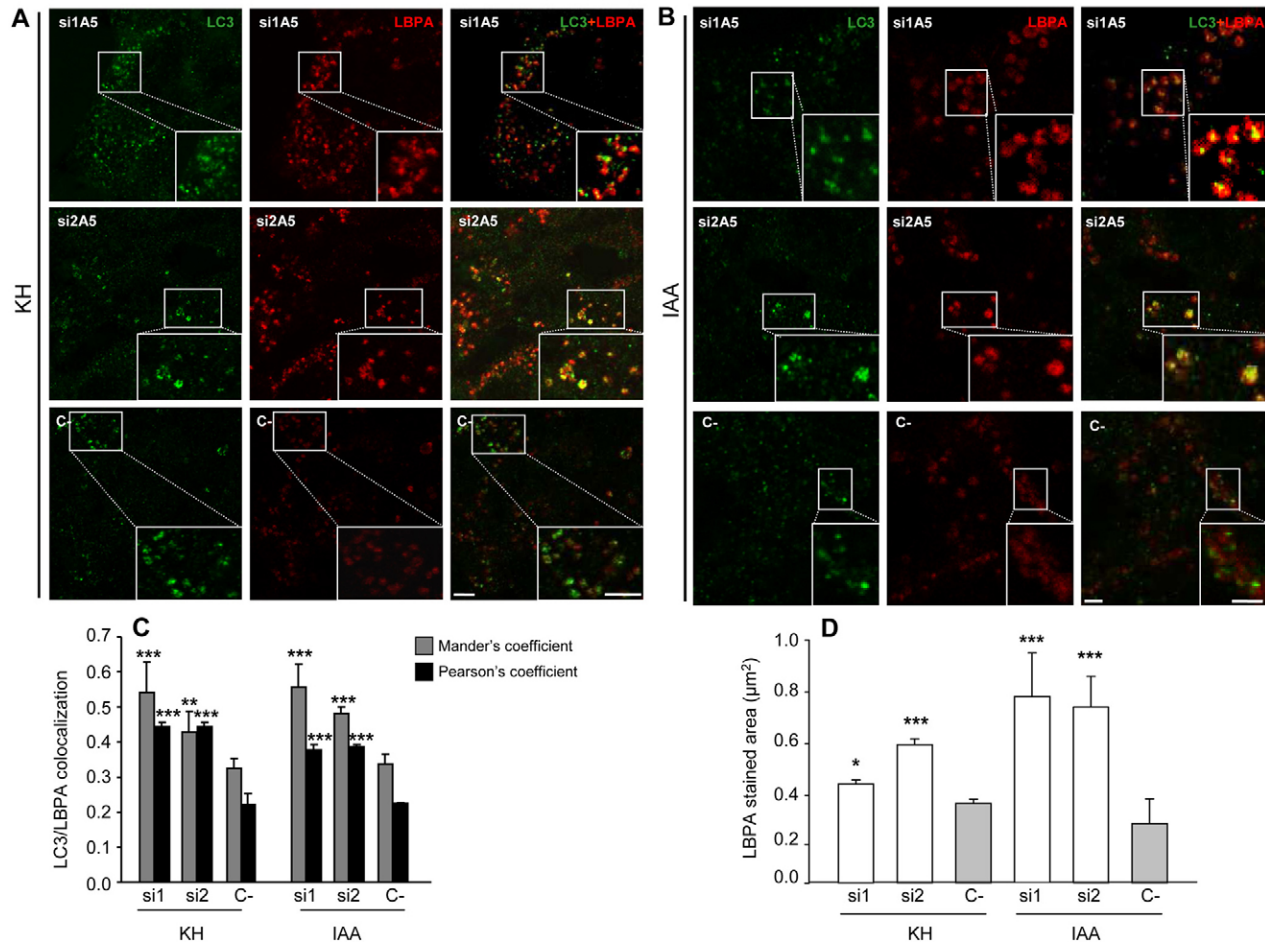
Fig. 11. Silencing of annexin A5 enhances autophagosome–endosome fusion. NIH3T3 cells were treated with two different annexin A5 siRNAs (si1A5 or si2A5) or with a negative control (C–) siRNA. (**A**,**B**) After 72 hours, the cells were incubated in KH (A) or in IAA (B) medium for 4 hours and immunostained with LBPA and LC3 antibodies. The cells were observed using a Leica confocal microscope. In A and B, first, second and third rows correspond, respectively, to cells treated with si1A5, si2A5 or C–, and right, middle and left panels show, respectively, LC3 (green fluorescence), LBPA (red fluorescence) immunostaining and the merge of both. The insets show high-magnification images of selected areas to show more clearly the colocalisations. Scale bars: 5 µm (A) and 2.5 µm (B). (**C**) Quantification of colocalisation of LC3 with LBPA. The analysis, from two independent experiments, was performed as detailed in the legend to Fig. 2E with the Mander's colocalisation coefficient (grey bars) showing the fraction of LC3-containing vesicles overlapping with LBPA-positive structures. (**D**) Quantification of LBPA (late endosomes)-stained areas in two independent experiments, using LCS Lite software under the conditions cited above. Differences from negative control (C–) values in C and D were found to be statistically significant at *$P<0.05$, **$P<0.005$ and ***$P<0.0005$.

protein from the Golgi complex to lysosomes and, to a much lesser extent, to late endosomes. Several reports have associated annexin A5 with the Golgi complex and the ER (Barwise and Walker, 1996; Rambotti et al., 1993), late endosomal membranes (Diakonova et al., 1997; Rambotti et al., 1993) and also with the nucleus (reviewed by Monastyrskaya et al., 2009). Our results do not show a significant nuclear localisation of annexin A5, probably because our experiments were carried out in the absence of serum, which appears to contain factors necessary for nuclear localisation (Barwise and Walker, 1996; Mohiti et al., 1997). We also did not find colocalisation of annexin A5 with the ER, probably because it is cell specific, because annexin A5 was located at the ER and Golgi complex in Langhans cells (Rambotti et al., 1993), but only at the Golgi complex in hepatoma cells (Gao et al., 2005).

We hypothesised that translocation of annexin A5 to the lysosomal membranes under starvation represents an important

mechanism in the control of autophagy and/or lysosomal degradation. This was found to be the case in pulse–chase experiments and in measurements of p62 levels after overexpressing or silencing annexin A5. These data, combined with results from LC3 western blots and eGFP–LC3 experiments, without lysosomal inhibitors and under both annexin A5 overexpression and silencing, suggest a main role of annexin A5 in autophagosome clearance. Fluorescence decay experiments together with mRFP–GFP–LC3 reporter data further support the proposal that annexin A5 is involved in the fusion of autophagosomes with lysosomes rather than in modifying the lysosomal degradative capacity, because no changes in lysosomal pH or in proteolytic activity at acid pHs were detected under knockdown and overexpression of this protein. This role of annexin A5 is compatible with previous indications that Ca^{2+}, together with the acid intralysosomal pH, are essential for autophagosome–lysosome fusion (Koga et al., 2010), and also with experiments

showing that annexin A5 induces *in vitro* fusion and aggregation of vesicles in a Ca^{2+}- and acidic-pH-dependent manner (Hoekstra et al., 1993). Indeed, annexin A5 binds to phospholipids in a Ca^{2+}-sensitive manner (Walker et al., 1992) and, because unpublished data from our laboratory show a rise of intracellular Ca^{2+} under starvation in mouse and human fibroblasts, it seems possible that it is this rise in Ca^{2+} that induces annexin A5 translocation to lysosomal membranes. In fact, colocalisation of annexin A5 with lysosomes increases with ionomycin treatment in IAA, whereas the well-established Ca^{2+} chelator BAPTA-AM, prevents this colocalisation in KH medium. Also, because amino acids decrease intracellular Ca^{2+} levels but insulin does not (our unpublished results), this could explain why, in contrast to amino acids, insulin does not reduce the binding of annexin A5 to lysosomal membranes. Hence, all these data are compatible with a requirement of Ca^{2+} for the translocation of annexin A5 to the lysosomal membranes. Moreover, annexin A5 shows a cholesterol-mediated enhancement of its Ca^{2+}-dependent binding to membranes (Ayala-Sanmartin, 2001), and the importance of membrane cholesterol levels in the fusion of lysosomes with autophagosomes has also been reported (Massey et al., 2008). Thus, annexin A5 could induce autophagosome–lysosome fusion through cholesterol-rich domains in their membranes in a pH- and Ca^{2+}-dependent way. However, the precise molecular mechanisms that drive these fusion events remain to be investigated.

The results obtained after annexin A5 silencing in the cells incubated with lysosomal inhibitors appear to be contradictory, because they still indicate higher levels of LC3-II. A possible explanation could be provided by the negative role of annexin A5 in both fluid phase and cholera toxin endocytosis. We propose that annexin A5 knockdown enhances both internalisation and convergence of endocytosis with the autophagic pathway. In fact, our data indicate a substantial increase in autophagosome–late endosome fusion to form amphisomes under the low levels of annexin A5 remaining after silencing. Previous reports have shown increased accumulation of amphisomes when fusion between autophagosomes and lysosomes is impaired (Eskelinen et al., 2002; Koga et al., 2010; Massey et al., 2008), which is consistent with our results. It is known that late endosomes have proteolysis competence, although it is less efficient than lysosomes (Pillay et al., 2002). Consistent with these observations, annexin A5 silencing will make degradation of LC3 in amphisomes less efficient, and this could explain the higher levels of the LC3-II autophagic marker observed under these conditions in the presence of protease inhibitors. Thus, we propose that the impairment of autophagosome fusion with lysosomes by annexin A5 knockdown is partially compensated for by an enhanced formation of amphisomes.

If this is so, an obvious question is how does annexin A5 negatively regulate the fusion of autophagosomes with late endosomes, while promoting the fusion with lysosomes. Our data show colocalisation of annexin A5 with lysosomes but also with late endosomes. Interestingly, a recent study suggests that, despite their similarities, fusion of autophagosomes with lysosomes or endosomes are distinctly governed, because the two types of fusion have different nucleotide requirements (Koga et al., 2010). Annexin A5 could differentially affect the fusion of the different organelles, enhancing the fusion of certain lipids and blocking others. The identification of the precise mechanisms by which annexin A5 is involved in the fusion machinery of autophagosomes with endosomes or with lysosomes will require

further work, but one possibility is that the observed differences are due to distinct intrinsic properties of the membranes of these compartments, determined by their lipid composition. Relevant to this study, annexin A1, another Ca^{2+}-binding protein with a substantial degree of biological and structural homology to annexin A5, has recently been related to autophagy regulation (Kang et al., 2011), and the authors propose that this occurs by controlling the formation of amphisomes. In our 2D-DIGE proteomic study, this protein was one of the three Ca^{2+}-dependent phospholipid-binding proteins (annexin A1, annexin A5 and copine 1) whose levels increased on lysosomal membranes from human fibroblasts under conditions of high proteolysis. Therefore, it is possible that there is some redundancy among these proteins in their effects on lysosomal degradation. In fact, we found that although cosilencing of annexin A5 and annexin A1 does not further increase the inhibition of lysosomal degradation produced by annexin A5 ($\sim$15%), cosilencing of annexin A5 and of copine I produces an important increase ($\sim$40%) in this inhibition.

In summary, our findings indicate new functions for annexin A5, promoting delivery of autophagosomes to lysosomes and inhibiting endocytosis. Therefore, annexin A5 emerges as a possible key positive regulator of autophagy and negative regulator of endocytosis through Ca^{2+} and phospholipid signalling pathways. It will be important to further investigate the molecular details of these mechanisms.

Materials and Methods

Reagents
Minimum essential medium (MEM), Dulbecco's modified Eagle's medium (DMEM), human insulin, fluorescein isothiocyanate (FITC)–dextran, azoalbumin, ionomycin, bafilomycin, 3-methyladenine and NH_4Cl were purchased from Sigma Chemical Co. MEM amino acids 50$\times$, foetal bovine serum, penicillin and streptomycin were supplied by Invitrogen Life Technologies, and LysoTracker Red, Alexa-Fluor-488–cholera-toxin-subunit-B and Alexa-Fluor-488–EGF were from Molecular Probes. Leupeptin was from Peptide Institute, Inc., saponin was from Merck and bovine serum albumin (BSA) from Roche Applied Science. BAPTA-AM was from Tocris. Metrizamide was from Nycomed and Percoll from Amersham Pharmacia Biotech Inc. The following antibodies were used: anti-annexin A5 and anti-cathepsin B from Santa Cruz Biotechnology; anti-LC3B from Nanotools; anti-LBPA from Echelon Biosciences Inc.; anti-lamin A, anti-p62 and anti-lamp 1 from Abcam; anti-β-actin and horseradish-peroxidase-labelled secondary antibodies from Sigma Chemical Co.; and anti-mitochondrial complex II (succinate-ubiquinol oxidoreductase, 70 kDa subunit) and Alexa-Fluor-488 and Alexa-Fluor-633-conjugated anti-rabbit and anti-mouse secondary antibodies from Molecular Probes (Invitrogen Life Technologies). Cell light-ER, Cell light-Golgi and Organelle light-early endosomes were purchased from Invitrogen Life Technologies. Radioisotopes were obtained from Invitrogen. Other reagents, purchased from Sigma Chemical Co, Invitrogen Life Technologies or Calbiochem, were of analytical grade.

Cell culture and general procedures
NIH3T3 (a mouse embryonic fibroblast cell line) and HEK293T (a human embryonic kidney cell line) cells were obtained from the European Collection of Animal Cell Cultures. Cells were grown at 37℃ in a humidified atmosphere of 5% CO_2/air (v/v) in MEM or DMEM, respectively, containing 10% foetal bovine serum and 1% penicillin–streptomycin. Krebs–Henseleit medium (KH; 18.4 mM NaCl, 4.75 mM KCl, 1.19 mM KH_2PO_4, 2.54 mM $MgSO_4$, 2.44 mM $CaCl_2 \cdot 2H_2O$, 28.6 mM $NaHCO_3$, 20 mM glucose) with 10 mM Hepes, pH 7.4, was used for high proteolysis (starvation) conditions. For low proteolysis conditions, insulin 0.1 μM (I), essential amino acids (AA) or both (IAA) at two times the concentration present in the growth media were added on KH medium. Cell viability and growth curves were determined in parallel for each culture.

For immunoblotting, we followed a standard procedure previously described (Fuertes et al., 2003a). Protein bands were quantified by densitometric analysis with an Image Quant ECL (GE Healthcare). Electron microscope morphometry and identification of Av_i and Av_d were carried out as described previously (Esteban et al., 2007; Knecht et al., 1984). Proteolytic activity in cell extracts was measured by a standard endopeptidase assay with azoalbumin (Sarath et al., 2001).

Proteolysis under in vitro conditions was also determined in radioactively labelled cell extracts as described previously (Vargas et al., 1989). Protein concentration was measured using a modified Lowry procedure, with sodium deoxycholate, and using bovine serum albumin as the standard.

Subcellular fractionation

After incubation in KH or in IAA, NIH3T3 cells were washed with phosphate-buffered saline (PBS) and pooled in ice-cold homogenisation buffer (250 mM sucrose, 20 mM Hepes, 1 mM EDTA, pH 7.4). Then, cells were homogenised at 4°C, first with a nitrogen cavitation pump (2.41×10^5 Pa, 7 minutes), and then with a tight-fitting Dounce homogeniser (10 strokes). A lysosomal fraction was prepared following a procedure described elsewhere (Storrie and Madden, 1990). Briefly, homogenates were centrifuged at 3000 g for 10 minutes at 4°C, the pellet was saved as the nuclear fraction and the post nuclear supernatant was applied to a Percoll–metrizamide gradient (from top to bottom: 6% Percoll; 17% and 35% metrizamide) and centrifuged at 53,000 g for 35 minutes at 4°C in an SW41Ti rotor (Beckman). To separate lysosomes from mitochondria, the 6% Percoll–17% metrizamide interface material was brought to 35% metrizamide and placed on the bottom of a second gradient of sucrose–metrizamide (from top to bottom: 0.25 M sucrose plus 5%, 17% and 35% metrizamide). After centrifugation at 53,000 g for 30 minutes, 4°C, mitochondria and lysosomes were collected from the 17%/35% and the 5%/17% metrizamide interfaces, respectively, and were disrupted by freezing and thawing, ten times. Lysosomal membranes were obtained by centrifugation at 105,000 g for 20 minutes at 4°C, in a Beckman Airfuge (rotor A-100), and washed three times.

Two-dimensional electrophoresis and mass spectroscopy

2D-DIGE of lysosomal membranes was carried out essentially as previously described (Bernal et al., 2006), solubilising protein samples purified as above in 7 M urea, 2 M thiourea, 4% (w/v) CHAPS, 20 mM dithiothreitol (DTT) and 2% (v/v) Biolytes 3–10 and Bromophenol Blue (all chemicals from Bio-Rad). Samples of 100 μg protein were subjected to isoelectric focusing generated on a Bio-Rad PROTEAN® IEF Cell at 20°C. Subsequently, the strips were reduced and alkylated (using 2.5% iodoacetamide and 2% DTT in succession) in equilibration buffer containing 6 M urea, 0.375 M Tris pH 8.8, 2% sodium dodecyl sulfate (SDS) and 20% glycerol. Polyacrylamide gels (10%) were employed for the second dimension. The spots observed in the gel were manually excised, washed twice with double distilled water and digested with sequencing grade trypsin (Promega) as described previously (Andresen et al., 1989). Proteins were identified by mass spectrometry using a 4700 Proteomics analyser (Applied Biosystems). A MASCOT search engine (Matrix-Science, London, UK) was used for a database search on SwissProt and NCBInr. The accuracy of proteins identification was considered when at least three peptides were identified with a minimum overall MASCOT score >50. The significance threshold for a change in proteins levels in the various conditions was set to $P \leq 0.05$ and the values were determined by factorial ANOVA tests using STATVIEW v4.53 (Abacus Concepts).

Measurements of intracellular protein degradation

Cells were incubated for 48 hours in full medium containing 2 μCi/ml [^{3}H]valine, washed and incubated for 24 hours in fresh full medium containing 10 mM L-valine to eliminate radiolabelled short-lived proteins (Fuertes et al., 2003b). Then, cells were incubated for the indicated times in KH or IAA medium. Total, lysosomal and autophagic protein degradations were measured and calculated as previously described (Fuertes et al., 2003a; Fuertes et al., 2003b).

Annexin A5 overexpression and small interfering RNA suppression

HEK293T cells were transiently transfected with An5-pCMV-Sport6 (annexin A5 overexpression vector; referred to as A5 vector), obtained from Open Biosystems, and empty pCMV-Sport6 or pCMV–GFP (negative control vectors: C– vector), obtained from Molecular Probes, Invitrogen Life Technologies. Transfections were carried out using Fugene HD (Roche Applied Science), according to the manufacturer's instructions. Experimental analyses of overexpression were started 48 hours after transfections. For RNAi-mediated inhibition of annexin A5 gene expression, cells were transfected, 72 hours before analysis, with small interfering RNAs (siRNAs), using X-tremeGENE siRNA Transfection Reagent (Roche Applied Science) for NIH3T3 cells and siLentFect Lipid Reagent (Bio-Rad) for NIH3T3 cells stably expressing eGFP–LC3 or mRFP–GFP–LC3, according to the manufacturer's instructions. NIH3T3 and HEK293 cells stably expressing eGFP–LC3 were generated by transfection with eGFP–LC3 (the construct was a kind gift from Tamotsu Yoshimori, Department of Genetics, Osaka University, Japan) and subsequent selection of eGFP–LC3 stable transformants in the presence of 1 mg/ml geneticin (Gibco).

Isolation of NIH3T3 and HEK293 cells stably expressing the mRFP–GFP–LC3 reporter (Kimura et al., 2007) was accomplished by transfecting the cells with mRFP–GFP–LC3 (purchased from Addgene), and submitting the resistant clones to two sequential cycles of cell sorting using a MoFlo high speed cell sorter (Beckman-Coulter). The steady-state expression level was then confirmed by

fluorescence-activated cell sorting (FACS), immunoblotting and confocal microscope analyses. These cells were grown in the same conditions as reported above (in the presence of 1 mg/ml geneticin). Two different siRNAs (1 and 2), purchased from Ambion Inc., that target mouse annexin A5 mRNA (hereafter siA5) were used at a final concentration of 25 nM, for NIH3T3 and HEK293T cells (in these human cells, annexin A5 knockdown was successful with mouse siRNA), and of 15 nM, for NIH3T3 with a stable expression of eGFP–LC3. A scrambled, non-targeting siRNA obtained from Ambion was used as a negative control (C–). Silencing efficiency was estimated at the protein level by western blotting.

Fluorescence microscopy

Cells were cultured on coverslips in 12-well plates. After the different treatments (KH or IAA), lysosomes were stained by incubation with 75 nM LysoTracker Red for 30 minutes at 37°C. Then, cells were rinsed with PBS, fixed with 3.7% paraformaldehyde–PBS for 20 minutes at room temperature, washed with PBS, and mounted using Fluor-Save reagent (Calbiochem). For immunofluorescence staining, cells were fixed as above, blocked with 0.1% BSA in PBS for 10 minutes and permeabilised with saponin (0.05% w/v in PBS) for 10 minutes. Then, cells were incubated with antibodies against annexin A5 (dilution 1:100), cathepsin B (dilution 1:100), LC3 (dilution 1:50) or LBPA (dilution 1:50). Bound antibodies were subsequently detected by incubation, as appropriate, with Alexa-Fluor-488-, 633- or 647-conjugated rabbit, mouse or goat secondary antibodies (dilution 1:200). ER, Golgi and early endosome fluorescent signals were obtained by transfecting the cells (following the manufacturer's instructions; Invitrogen) with Cell Light-ER (endoplasmic signal sequence of calreticulin and KDEL–RFP), Cell Light-Golgi (N-acetylgalactosaminyl-transferase 2–RFP) and Organelle Light-early endosomes (Rab5a–RFP). Preparations were observed with a Leica DM6000 B fluorescence microscope and images were acquired with a Leica TC5 confocal laser scanning microscope. Laser lines were 488 nm (eGFP–LC3, RFP–GFP–LC3 and Alexa Fluor 488), 561 nm (RFP–GFP–LC3) and 633 and 647 nm (Alexa Fluor 633 and 647). The JaCoP plug-in (Bolte and Cordelieres, 2006) in ImageJ software was used for the quantification of the various colocalisations. The eGFP–LC3 (autophagosomes)- and LysoTracker Red (lysosomes)-stained areas were quantified using LCS Lite software. The number of eGFP–LC3 puncta was counted using the Top Hat algorithm in MetaMorph version 7.0.

Measurement of lysosomal pH

To measure the pH within lysosomes, cells were allowed to endocytose FITC-conjugated dextran, following a procedure described elsewhere (Nilsson et al., 2003). Briefly, 72 or 48 hours after annexin A5 knockdown or overexpression, respectively, cells seeded in 12-well plates were treated with 40 kDa FITC–dextran (0.5 mg/ml) for 18 hours. Cells were then washed five times with PBS and incubated in KH or IAA medium for 4 hours to chase the FITC–dextran from the endosomes. Positive control samples were incubated with NH_4Cl (20 mM). Cells were then resuspended and washed three times in fresh KH or IAA medium after being transferred to FACS tubes. Cell pellets were kept on ice and resuspended immediately before FACS analysis. FITC was excited at 488 nm with an argon laser and the resulting emission was detected using a 530±28 nm (FL1) and a 610±20 nm (FL3) filter. The FL1/FL3 ratios were measured for 5000 collected cells, and pH was calculated using a standard curve prepared with McIlvaine's buffers (pHs ranging from 4.0 to 6.0), containing sodium azide (50 mM), 2-deoxyglucose (50 mM), nigericin (10 μM) and monensin (20 μM).

Flow cytometry

Lysosomal mass was determined by incubating the cells in suspension (10^6 cells/ml) with 75 nM LysoTracker Red for 30 minutes at 37°C, and the emitted red fluorescence (620±20 nm band-pass filter) was analyzed (Poot, 2001). For detection of fluid phase endocytosed cargo, using flow cytometry, cells were treated with FITC–dextran (1 mg/ml) for 30, 60 or 120 minutes at 37°C. For detection of endocytosis of cholera toxin B or epidermal growth factor (EGF), cells were treated with Alexa-Fluor-488–cholera-toxin-subunit-B (1.5 μg/ml) or with Alexa-Fluor-488–EGF (2 μg/ml) for 5, 15, 30, 60 or 90 minutes at 37°C. Previously, cells were also incubated as above for 5 seconds at 4°C to evaluate the membrane-bound marker. At the different times, cells were detached with trypsin–EDTA, washed four times, resuspended in PBS (10^6 cells/ml), and the emitted red (620±20 nm band-pass filter) or green (488±20 nm band-pass filter) fluorescences were analyzed by flow cytometry. In each experiment, 10,000 cells were collected and analyzed using a Cytomics FC 500 flow cytometer (Beckman Coulter). Autophagy quantification by flow cytometry was determined by a procedure described elsewhere (Shvets and Elazar, 2009).

Quantification and statistics

P-values were determined by factorial ANOVA tests using GraphPad Prism software. P-values are indicated in all figures by asterisks: ***P<0.0005, **P<0.005 and *P<0.05.

Supplementary material available online at
http://jcs.biologists.org/lookup/suppl/doi:10.1242/jcs.086728/-/DC1

References

Andresen, K., Simonsen, P. E., Andersen, B. J. and Birch-Andersen, A. (1989). Echinostoma caproni in mice: shedding of antigens from the surface of an intestinal trematode. *Int. J. Parasitol.* **19**, 111-118.

Axe, E. L., Walker, S. A., Manifava, M., Chandra, P., Roderick, H. L., Habermann, A., Griffiths, G. and Ktistakis, N. T. (2008). Autophagosome formation from membrane compartments enriched in phosphatidylinositol 3-phosphate and dynamically connected to the endoplasmic reticulum. *J. Cell Biol.* **182**, 685-701.

Ayala-Sanmartin, J. (2001). Cholesterol enhances phospholipid binding and aggregation of annexins by their core domain. *Biochem. Biophys. Res. Commun.* **283**, 72-79.

Barwise, J. L. and Walker, J. H. (1996). Subcellular localization of annexin V in human foreskin fibroblasts: nuclear localization depends on growth state. *FEBS Lett.* **394**, 213-216.

Bernal, D., Carpena, I., Espert, A. M., De la Rubia, J. E., Esteban, J. G., Toledo, R. and Marcilla, A. (2006). Identification of proteins in excretory/secretory extracts of Echinostoma friedi (Trematoda) from chronic and acute infections. *Proteomics* **6**, 2835-2843.

Berridge, M. J., Bootman, M. D. and Roderick, H. L. (2003). Calcium signalling: dynamics, homeostasis and remodelling. *Nat. Rev. Mol. Cell Biol.* **4**, 517-529.

Bolte, S. and Cordelieres, F. P. (2006). A guided tour into subcellular colocalization analysis in light microscopy. *J. Microsc.* **224**, 213-232.

Cederholm, A. and Frostegard, J. (2007). Annexin A5 multitasking: a potentially novel antiatherothrombotic agent? *Drug News Perspect.* **20**, 321-326.

Codogno, P. and Meijer, A. J. (2005). Autophagy and signaling: their role in cell survival and cell death. *Cell Death Differ.* **12**, Suppl. 2, 1509-1518.

Cuervo, A. M. (2010). The plasma membrane brings autophagosomes to life. *Nat. Cell Biol.* **12**, 735-737.

Diakonova, M., Gerke, V., Ernst, J., Liautard, J. P., van der Vusse, G. and Griffiths, G. (1997). Localization of five annexins in J774 macrophages and on isolated phagosomes. *J. Cell Sci.* **110**, 1199-1213.

Douglas, P. M. and Dillin, A. (2010). Protein homeostasis and aging in neurodegeneration. *J. Cell Biol.* **190**, 719-729.

Eskelinen, E. L., Illert, A. L., Tanaka, Y., Schwarzmann, G., Blanz, J., von Figura, K. and Saftig, P. (2002). Role of LAMP-2 in lysosome biogenesis and autophagy. *Mol. Biol. Cell* **13**, 3355-3368.

Esteban, I., Aguado, C., Sanchez, M. and Knecht, E. (2007). Regulation of various proteolytic pathways by insulin and amino acids in human fibroblasts. *FEBS Lett.* **581**, 3415-3421.

Esteve, J. M., Armengod, M. E. and Knecht, E. (2010). BRCA1 negatively regulates formation of autophagic vacuoles in MCF-7 breast cancer cells. *Exp. Cell Res.* **316**, 2618-2629.

Fuertes, G., Martin De Llano, J. J., Villarroya, A., Rivett, A. J. and Knecht, E. (2003a). Changes in the proteolytic activities of proteasomes and lysosomes in human fibroblasts produced by serum withdrawal, amino-acid deprivation and confluent conditions. *Biochem. J.* **375**, 75-86.

Fuertes, G., Villarroya, A. and Knecht, E. (2003b). Role of proteasomes in the degradation of short-lived proteins in human fibroblasts under various growth conditions. *Int. J. Biochem. Cell Biol.* **35**, 651-664.

Gao, C. X., Miyoshi, E., Uozumi, N., Takamiya, R., Wang, X., Noda, K., Gu, J., Honke, K., Wada, Y. and Taniguchi, N. (2005). Bisecting GlcNAc mediates the binding of annexin V to Hsp47. *Glycobiology* **15**, 1067-1075.

Gordon, P. B., Holen, I., Fosse, M., Rotnes, J. S. and Seglen, P. O. (1993). Dependence of hepatocytic autophagy on intracellularly sequestered calcium. *J. Biol. Chem.* **268**, 26107-26112.

Hailey, D. W., Rambold, A. S., Satpute-Krishnan, P., Mitra, K., Sougrat, R., Kim, P. K. and Lippincott-Schwartz, J. (2010). Mitochondria supply membranes for autophagosome biogenesis during starvation. *Cell* **141**, 656-667.

Hayashi-Nishino, M., Fujita, N., Noda, T., Yamaguchi, A., Yoshimori, T. and Yamamoto, A. (2009). A subdomain of the endoplasmic reticulum forms a cradle for autophagosome formation. *Nat. Cell Biol.* **11**, 1433-1437.

Hoekstra, D., Buist-Arkema, R., Klappe, K. and Reutelingsperger, C. P. (1993). Interaction of annexins with membranes: the N-terminus as a governing parameter as revealed with a chimeric annexin. *Biochemistry* **32**, 14194-14202.

Hoyer-Hansen, M., Bastholm, L., Szyniarowski, P., Campanella, M., Szabadkai, G., Farkas, T., Bianchi, K., Fehrenbacher, N., Elling, F., Rizzuto, R. et al. (2007). Control of macroautophagy by calcium, calmodulin-dependent kinase kinase-beta, and Bcl-2. *Mol. Cell* **25**, 193-205.

Kang, J. H., Li, H., Chen, X. and Yin, X. M. (2011). Proteomics analysis of starved cells revealed Annexin A1 as an important regulator of autophagic degradation. *Biochem. Biophys. Res. Commun.* **407**, 581-586.

Kimura, S., Noda, T. and Yoshimori, T. (2007). Dissection of the autophagosome maturation process by a novel reporter protein, tandem fluorescent-tagged LC3. *Autophagy* **3**, 452-460.

Klionsky, D. J., Cregg, J. M., Dunn, W. A., Jr, Emr, S. D., Sakai, Y., Sandoval, I. V., Sibirny, A., Subramani, S., Thumm, M., Veenhuis, M. et al. (2003). A unified nomenclature for yeast autophagy-related genes. *Dev. Cell* **5**, 539-545.

Knecht, E., Hernandez-Yago, J. and Grisolia, S. (1984). Regulation of lysosomal autophagy in transformed and non-transformed mouse fibroblasts under several growth conditions. *Exp. Cell Res.* **154**, 224-232.

Knecht, E., Aguado, C., Carcel, J., Esteban, I., Esteve, J. M., Ghislat, G., Moruno, J. F., Vidal, J. M. and Saez, R. (2009). Intracellular protein degradation in mammalian cells: recent developments. *Cell. Mol. Life Sci.* **66**, 2427-2443.

Koga, H., Kaushik, S. and Cuervo, A. M. (2010). Altered lipid content inhibits autophagic vesicular fusion. *FASEB J.* **24**, 3052-3065.

Kornhuber, J., Henkel, A. W., Groemer, T. W., Stadtler, S., Welzel, O., Tripal, P., Rotter, A., Bleich, S. and Trapp, S. (2010). Lipophilic cationic drugs increase the permeability of lysosomal membranes in a cell culture system. *J. Cell. Physiol.* **224**, 152-164.

Levine, B. and Klionsky, D. J. (2004). Development by self-digestion: molecular mechanisms and biological functions of autophagy. *Dev. Cell* **6**, 463-477.

Lum, J. J., Bauer, D. E., Kong, M., Harris, M. H., Li, C., Lindsten, T. and Thompson, C. B. (2005). Growth factor regulation of autophagy and cell survival in the absence of apoptosis. *Cell* **120**, 237-248.

Luzio, J. P., Bright, N. A. and Pryor, P. R. (2007). The role of calcium and other ions in sorting and delivery in the late endocytic pathway. *Biochem. Soc. Trans.* **35**, 1088-1091.

Mari, M., Griffith, J., Rieter, E., Krishnappa, L., Klionsky, D. J. and Reggiori, F. (2010). An Atg9-containing compartment that functions in the early steps of autophagosome biogenesis. *J. Cell Biol.* **190**, 1005-1022.

Massey, A. C., Follenzi, A., Kiffin, R., Zhang, C. and Cuervo, A. M. (2008). Early cellular changes after blockage of chaperone-mediated autophagy. *Autophagy* **4**, 442-456.

Meijer, A. J. and Codogno, P. (2006). Signalling and autophagy regulation in health, aging and disease. *Mol. Aspects Med.* **27**, 411-425.

Mizushima, N., Yoshimori, T. and Levine, B. (2010). Methods in mammalian autophagy research. *Cell* **140**, 313-326.

Mohiti, J., Caswell, A. M. and Walker, J. H. (1997). The nuclear location of annexin V in the human osteosarcoma cell line MG-63 depends on serum factors and tyrosine kinase signaling pathways. *Exp. Cell Res.* **234**, 98-104.

Monastyrskaya, K., Babiychuk, E. B. and Draeger, A. (2009). The annexins: spatial and temporal coordination of signaling events during cellular stress. *Cell. Mol. Life Sci.* **66**, 2623-2642.

Moscat, J. and Diaz-Meco, M. T. (2009). p62 at the crossroads of autophagy, apoptosis, and cancer. *Cell* **137**, 1001-1004.

Nilsson, C., Kagedal, K., Johansson, U. and Ollinger, K. (2003). Analysis of cytosolic and lysosomal pH in apoptotic cells by flow cytometry. *Methods Cell Sci.* **25**, 185-194.

Noda, T., Fujita, N. and Yoshimori, T. (2009). The late stages of autophagy: how does the end begin? *Cell Death Differ.* **16**, 984-990.

Onodera, J. and Ohsumi, Y. (2005). Autophagy is required for maintenance of amino acid levels and protein synthesis under nitrogen starvation. *J. Biol. Chem.* **280**, 31582-31586.

Perez-Terzic, C. M., Chini, E. N., Shen, S. S., Dousa, T. P. and Clapham, D. E. (1995). Ca^{2+} release triggered by nicotinate adenine dinucleotide phosphate in intact sea urchin eggs. *Biochem. J.* **312**, 955-959.

Pillay, C. S., Elliott, E. and Dennison, C. (2002). Endolysosomal proteolysis and its regulation. *Biochem. J.* **363**, 417-429.

Poot, M. (2001). Analysis of intracellular organelles by flow cytometry or microscopy. *Curr. Protoc. Cytom.* **9**, Unit 9.4, pp. 1-24.

Pryor, P. R., Mullock, B. M., Bright, N. A., Gray, S. R. and Luzio, J. P. (2000). The role of intraorganellar Ca(2+) in late endosome-lysosome heterotypic fusion and the reformation of lysosomes from hybrid organelles. *J. Cell Biol.* **149**, 1053-1062.

Rambotti, M. G., Spreca, A. and Donato, R. (1993). Immunocytochemical localization of annexins V and VI in human placentae of different gestational ages. *Cell. Mol. Biol. Res.* **39**, 579-588.

Ravikumar, B., Moreau, K., Jahreiss, L., Puri, C. and Rubinsztein, D. C. (2010). Plasma membrane contributes to the formation of pre-autophagosomal structures. *Nat. Cell Biol.* **12**, 747-757.

Russo-Marie, F. (1999). Annexin V and phospholipid metabolism. *Clin. Chem. Lab. Med.* **37**, 287-291.

Sarath, G., Zeece, M. G., and Penheiter, A. R. (2001). Protease assay methods. In *Proteolytic Enzymes: a Practical Approach* (ed. R. Benyon and J. S. Bond), pp. 45-76. Oxford: Oxford University Press.

Shvets, E. and Elazar, Z. (2009). Flow cytometric analysis of autophagy in living mammalian cells. *Methods Enzymol.* **452**, 131-141.

Storrie, B. and Madden, E. A. (1990). Isolation of subcellular organelles. *Methods Enzymol.* **182**, 203-225.

Vargas, J. L., Aniento, F., Cervera, J. and Knecht, E. (1989). Vanadate inhibits degradation of short-lived, but not of long-lived, proteins in L-132 human cells. *Biochem. J.* **258**, 33-40.

Walker, J. H., Boustead, C. M., Koster, J. J., Bewley, M. and Waller, D. A. (1992). Annexin V, a calcium-dependent phospholipid-binding protein. *Biochem. Soc. Trans.* **20**, 828-833.

Williams, A., Sarkar, S., Cuddon, P., Ttofi, E. K., Saiki, S., Siddiqi, F. H., Jahreiss, L., Fleming, A., Pask, D., Goldsmith, P. et al. (2008). Novel targets for Huntington's disease in an mTOR-independent autophagy pathway. *Nat. Chem. Biol.* **4**, 295-305.

Wu, Y. T., Tan, H. L., Shui, G., Bauvy, C., Huang, Q., Wenk, M. R., Ong, C. N., Codogno, P. and Shen, H. M. (2010). Dual role of 3-methyladenine in modulation of autophagy via different temporal patterns of inhibition on class I and III phosphoinositide 3-kinase. *J. Biol. Chem.* **285**, 10850-10861.

Xie, Z. and Klionsky, D. J. (2007). Autophagosome formation: core machinery and adaptations. *Nat. Cell Biol.* **9**, 1102-1109.

Yla-Anttila, P., Vihinen, H., Jokitalo, E. and Eskelinen, E. L. (2009). 3D tomography reveals connections between the phagophore and endoplasmic reticulum. *Autophagy* **5**, 1180-1185.

Table S1. Lysosomal pH under annexin A5 overexpression and silencing

		Overexpression		Silencing
KH	C-	5.52±0.02	C-	5.66±0.08
	A5	5.58±0.10	siA5	5.64±0.02
	NH_4Cl	6.64±0.05	NH_4Cl	6.40±0.03
IAA	C-	5.23±0.07	C-	5.39±0.07
	A5	5.27±0.04	siA5	5.42±0.05
	NH_4Cl	6.38±0.11	NH_4Cl	6.49±0.14

HEK293T cells were transfected with C- or A5 vectors (for overexpression) or C- and siA5 (for silencing). After 48 or 72 h, respectively, lysosomal pH was measured in cells incubated in KH or IAA media for 4 h as described in Materials and Methods. NH_4Cl (20 mM) was used as positive control and pH values are shown as mean and s.d. from three different experiments. Differences were found not to be statistically significant.